iScience

CellPress
OPEN ACCESS

Article

Attenuating iPSC reprogramming stress with dominant-negative BET peptides

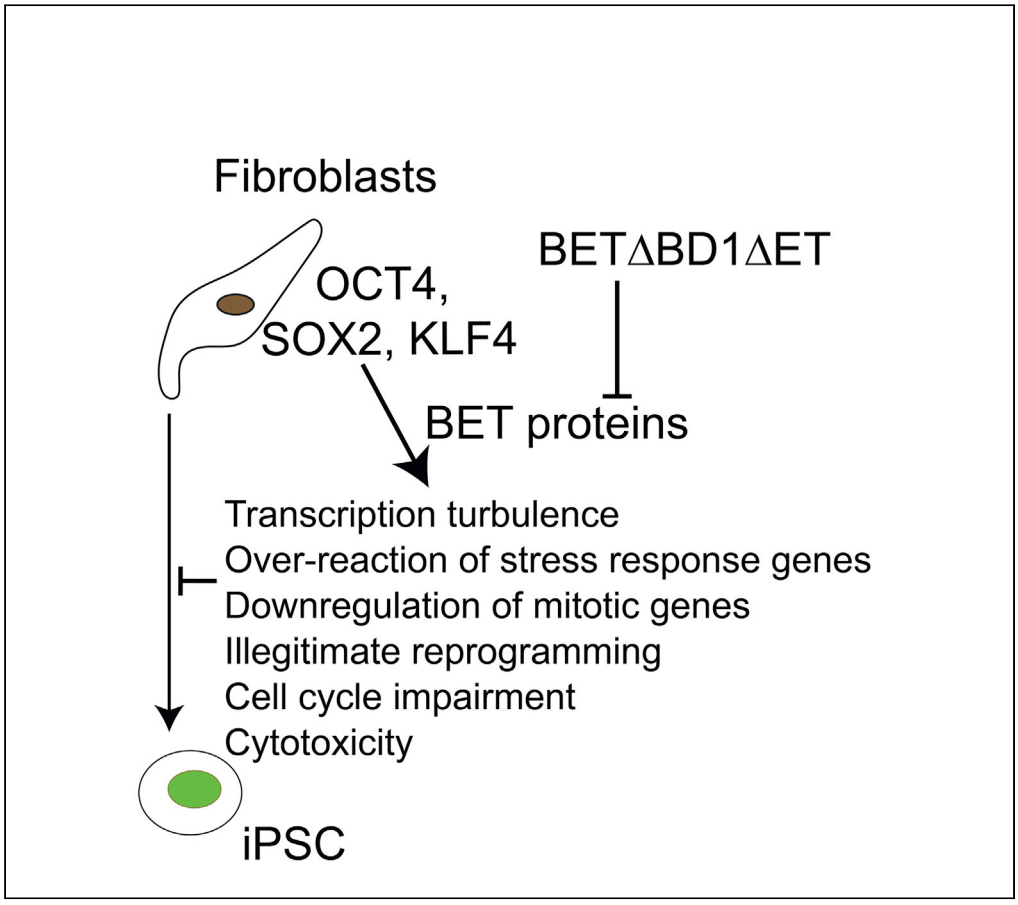

Md Emon Hossain, Ricardo Raul Cevallos, Ruowen Zhang, Kejin Hu

hukejin@gmail.com

Highlights

BET mini proteins of BRD2, BRD3, and BRD4 enhance iPSC reprogramming

BET mini proteins are dominant negative mimicking BET chemical inhibitors

OSK elicit reprogramming stresses at both molecular and cellular levels

BET mini proteins mitigate the OSK-elicited reprogramming stresses

Hossain et al., iScience *26*, 105889
January 20, 2023
https://doi.org/10.1016/j.isci.2022.105889

iScience

CellPress
OPEN ACCESS

Article

Attenuating iPSC reprogramming stress with dominant-negative BET peptides

Md Emon Hossain,[1,2] Ricardo Raul Cevallos,[1,2] Ruowen Zhang,[1] and Kejin Hu[1,3,*]

SUMMARY

Generation of induced pluripotent stem cells (iPSCs) is inefficient and stochastic. The underlying causes for these deficiencies are elusive. Here, we showed that the reprogramming factors (OCT4, SOX2, and KLF4, collectively OSK) elicit dramatic reprogramming stress even without the pro-oncogene MYC including massive transcriptional turbulence, massive and random deregulation of stress-response genes, cell cycle impairment, downregulation of mitotic genes, illegitimate reprogramming, and cytotoxicity. The conserved dominant-negative (DN) peptides of the three ubiquitous human bromodomain and extraterminal (BET) proteins enhanced iPSC reprogramming and mitigated all the reprogramming stresses mentioned above. The concept of reprogramming stress developed here affords an alternative avenue to understanding and improving iPSC reprogramming. These DN BET fragments target a similar set of the genes as the BET chemical inhibitors do, indicating a distinct approach to targeting BET proteins.

INTRODUCTION

A combination of four transcription factors (OCT4, SOX2, KLF4, and MYC, collectively OSKM) can convert many types of mammalian somatic cells into induced pluripotent stem cells (iPSCs).[1,2] iPSCs are man-made embryonic stem cells (ESCs) since they are very similar to each other in cell morphology, colony morphology, transcriptome, epigenetics landscape, culture requirements, self-renewal, and differentiation potentials.[3,4] However, iPSC reprogramming is very inefficient, stochastic, and slow, and leads to many undesired alternative fates.[4,5] The molecular underpinnings behind the stochastic and inefficient natures of iPSC reprogramming are poorly understood. It is long thought that intrinsic molecular barriers are the main reasons for the extremely low efficiency of iPSC reprogramming.[6] However, many types of cellular stress have been reported for the reprogramming cells.[7–15] *MYC* is a robust pro-oncogene and its overexpression causes oncogene stress.[16,17] iPSCs can be generated without MYC (OSK reprogramming) but the reprogramming efficiency becomes even lower.[18–20] Without MYC, mouse reprogramming cells still undergo replication stress albeit to a lesser degree.[9] Nevertheless, a concept of general reprogramming stress has not been established formally.

Bromodomain and extraterminal (BET) proteins are characterized by two tandem bromodomains (BD) in their N-termini and one extraterminal (ET) domain at their carboxyl termini. Each of their two bromodomains harbors an acetyllysine binding pocket. BET proteins bind to the acetylated histone tails via their bromodomains, and thus positively regulate transcription.[21] The mammalian BET family includes four members and three of them (BRD2, BRD3, and BRD4) are expressed ubiquitously. BET proteins regulate many cellular processes[21,22] including stress responses.[23–28] Mouse BRD4 was reported to promote murine iPSC reprogramming,[29] but inhibition of BET proteins promotes mouse neuron reprogramming.[30] By library screening, our laboratory discovered that BRD3R, a short isoform of human BRD3, enhances human iPSC reprogramming and mitotic activities of the reprogramming cells,[19] and that mild chemical inhibition of BET proteins promotes pluripotency reprogramming and dampens somatic transcription of the reprogramming cells.[18] These data indicate critical roles of BET proteins in reprogramming, but the exact underlying molecular mechanisms are elusive.

Here, we provide evidence that the Yamanaka reprogramming even in the absence of the pro-oncogene MYC causes significant reprogramming stress including massive transcriptional turbulence, massive and random dysregulation of stress-response genes, illegitimate upreprogramming, cell cycle impairment, downregulation of mitotic genes, and cytotoxicity. We further demonstrated that a series of BET

[1]Department of Biochemistry and Molecular Genetics, School of Medicine, University of Alabama at Birmingham, Birmingham, AL 35294, USA

[2]These authors contributed equally

[3]Lead contact

*Correspondence: hukejin@gmail.com

https://doi.org/10.1016/j.isci.2022.105889

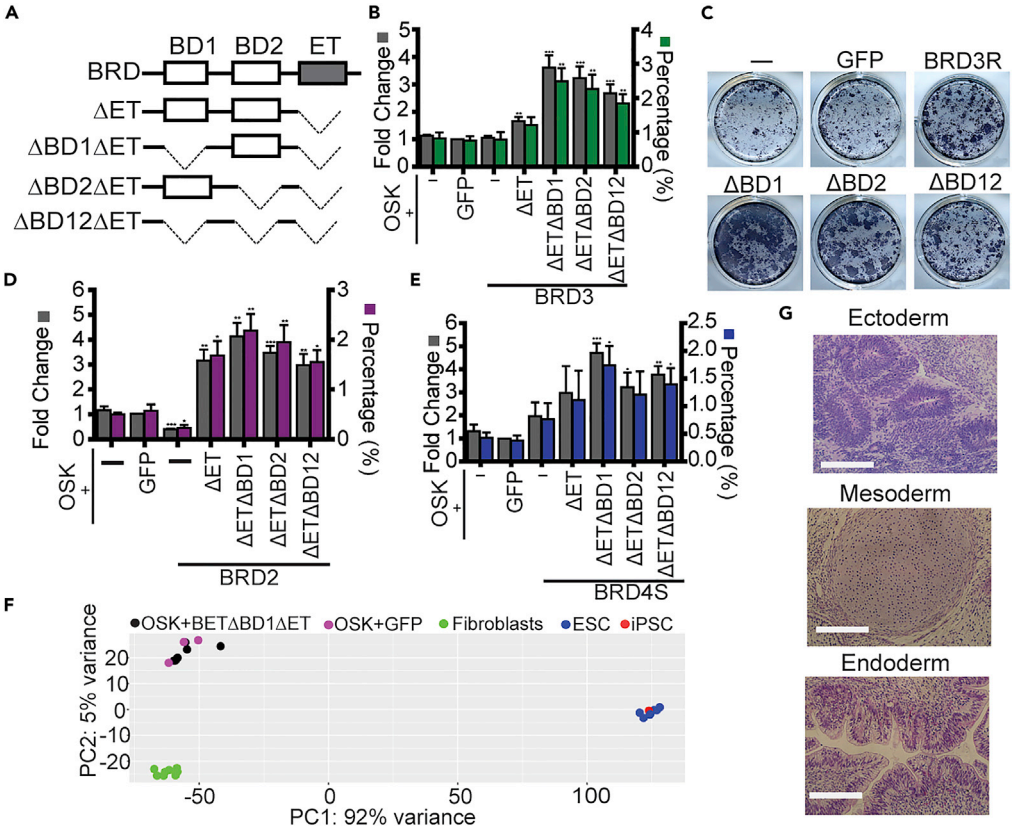

Figure 1. Conserved and masked reprogramming activities of human BET proteins independent of the characteristic bromodomains and ET domain

(A) Schematic representations for the deletion constructs of BET proteins. ΔBD12 denotes double deletion, i.e., ΔBD1ΔBD2.

(B, D, and E) Relative reprogramming activities of BRD3 (B), BRD2 (D), and BRD4S (E) deletion constructs. FC, fold changes (left Y axis); right Y axis is percentage of reprogramming. Student unpaired two-sided t-tests, n = 3 for BRD4; n = 4 for BRD2; n = 6 for BRD3. *, $p < 0.05$; **, $p < 0.01$; ***, $p < 0.001$.

(C) Representative images for ALP staining of the reprogramming wells for different BRD3R constructs under the OSK conditions. Additional transgenes are indicated above each panel. The lower row is for BRD3R deletion constructs.

(F and G) Human iPSCs generated by BET deletion mutants are pluripotent as shown by PCA (F) and teratoma tests (G). Bars, 200 μm. See also Figures S1–S4, S10, and S11.

dominant-negative (DN) deletion proteins of human BRD2, BRD3, and BRD4 attenuate all the above reprogramming stress and enhance human pluripotency reprogramming.

RESULTS

Masked reprogramming activity of human BRD3

We previously reported that the short isoform of human BRD3, BRD3R, enhanced pluripotency reprogramming while the conventional BRD3 did not.[19] The critical and characteristic BET domains are the double tandem bromodomains (BD1 and BD2) responsible for their binding to the acetylated chromatin[21] (Figures 1A, S1A, and S1C). Given their functional importance, we hypothesized that the BRD3R bromodomains are required for its reprogramming activity. To test this, we mutated the key residues for acetyllysine binding (YF mutations in Figure S1A). To our surprise, none of these YF mutations eliminated BRD3R reprogramming activity, but some increased reprogramming activities were observed (Figures S1B and S1E). Although the YF point mutations impair acetyllysine binding, those mutations do not eliminate BET binding to chromatin.[31] We therefore generated more dramatic deletions of BRD3R. The ZA loop within the bromodomain constitutes the acetyllysine binding packet of the BET bromodomain,[32] and we therefore deleted the ZA loops in each and both bromodomains (Figure S1C). These loop-deleted BRD3R still retained its reprogramming activities (Figure S1D). We then deleted the entire bromodomain individually or

together (Figure 1A), and the complete deletion of bromodomains resulted in even higher reprogramming activities as compared to their parental BRD3R (Figures 1B and 1C). These observations indicate that BRD3 harbors concealed reprogramming activity inhibited intramolecularly by its ET and bromodomains. Interestingly, we consistently observed a more robust inhibition by BD1 than BD2 and slight decrease in reprogramming activity for ΔBD1ΔBD2ΔET deletion as compared to the individual deletion of each bromodomain (Figures 1B and 1C) although those differences in mean values did not pass the significant test.

Masked BET reprogramming activities are conserved

There are three ubiquitous human BET proteins, BRD2, BRD3, and BRD4. We generated BRD2 and BRD4 counterparts of BRD3R by deleting the C-terminal tails containing the conserved ET domains (Figures 1A and S2A). Like BRD3R, both BRD2ΔET and BRD4SΔET gained reprogramming activities (Figures 1D, 1E, S2B, and S2C). We then additionally deleted individual and both bromodomains from BRD2ΔET and BRD4SΔET (Figures 1A, S2D, and S2F). Again, individual deletion of BD1 consistently displayed higher mean fold changes in reprogramming for both BRD2 and BRD4S although the differences in mean values did not pass the statistics test (Figures 1D, 1E, S2E, and S2G). Individual deletion of BD2 from BRD2ΔET and BRD4SΔET retained the reprogramming activities (Figures 1D, 1E, S2E, and S2G). Like BRD3R, double deletion of bromodomains from BRD2ΔET insignificantly but consistently compromised reprogramming activity as compared to individual deletion in our experiences (Figures 1B, 1D, and S2E). Interestingly, deletion of both bromodomains from BRD4SΔET did not impair its reprogramming activity (Figures 1E and S2G). We also tested whether a deletion of bromodomains alone can enhance reprogramming. Unlike ET tails, deletion of bromodomains alone did not confer the BET proteins reprogramming activities and the BD1 deletion even compromised reprogramming (Figure S3). In summary, the ubiquitous BET proteins all harbor reprogramming activities masked mainly by their ET-containing C-termini and additionally by their bromodomains, mainly BD1.

The BETΔBD1ΔET iPSCs established in this study have a normal karyotype (Figure S4C), and are pluripotent based on surface marker expression (TRA-1-60, TRA-1-81, SSEA3, SSEA4, and ALP, Figure S4B), expression of the pluripotency master regulators (OCT4, SOX2, NANOG, and LIN28, Figure S4A), teratoma tests (Figure 1G), and PCA clustering of transcriptomes (Figure 1F). Transgene silencing in iPSC is an indication of complete reprogramming. All of our reprogramming factors are constructed to co-express GFP.[19,33] The established iPSCs have silenced all the multiple copies of the co-expressed GFP (Figure S4D).

We also used the non-integrating Sendai reprogramming system along with BRD2ΔBD1ΔET and found that BRD2ΔBD1ΔET enhanced reprogramming as observed with the lentiviral reprogramming method (Figure S10).

We used additional pluripotent markers to test the reprogramming activities of BET deletion proteins. With TRA-1-60 as a pluripotency marker,[34] we found that the ΔBD1ΔET-deleted mini-proteins of BRD2, BRD3, and BRD4S all enhanced pluripotency reprogramming as compared to GFP (Figures S10 and S11). The percentage of reprogramming can be enhanced from 0.28% to 0.85%. We also stained the reprogramming colonies with the NANOG antibodies and these DN deletion proteins enhanced reprogramming as judged by number of $NANOG^+$ colonies (Figure S11C).

Legitimate reprogramming by the BET peptides

Next, we explored the underlying molecular mechanisms for the reprogramming activities in the BETΔBDΔET fragments released from their wild-type parental proteins. We recently developed and employed the concept of reprogramming legitimacy.[35–38] To evaluate the legitimacy of reprogramming by the BET deletion fragments, we sequenced RNA samples (RNA-seq) on the reprogramming cells. All the mutated and wild-type BET constructs were well expressed (Figures S5 and S6A, and data not shown). Downregulation of genes by all 3 BETΔBD1ΔET fragments was predominant (Figure S6B). This agrees with the positive roles of BET proteins in gene transcription if these BET deletion versions are considered as DN copies of BET proteins (see below). However, upregulation of genes by all the three BETΔBD1ΔET fragments was still substantial. This is not surprising since JQ1 treatment of the same starting cells under similar reprogramming conditions also upregulated a set of genes.[18] On the other hand, the wild-type BRD2 and BRD4S upregulated more genes than downregulation (Figure S6B) in agreement with their positive roles in transcription, but overexpression of the wild-type counterparts overall had much less impact on gene expression profiles (Figure S6B) than their DN counterparts.

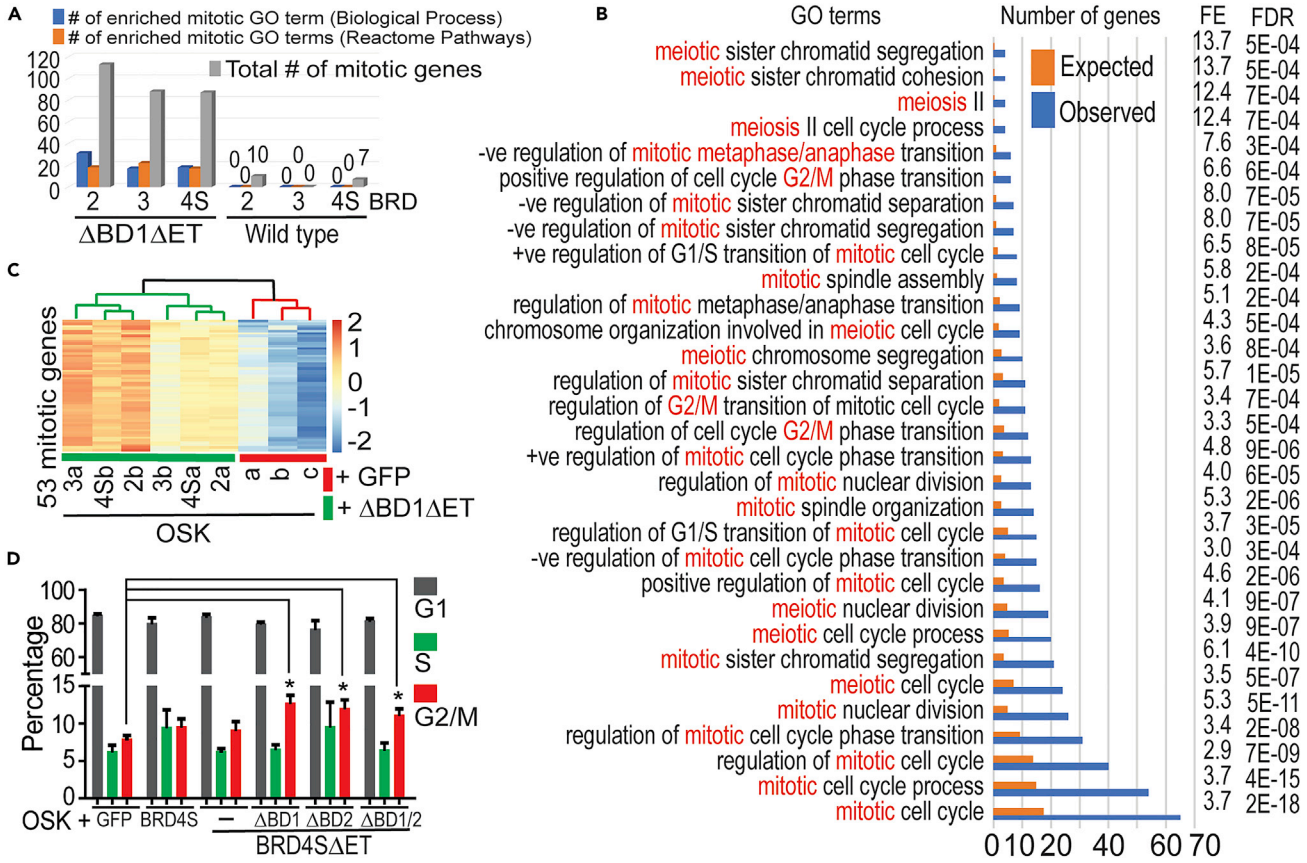

Figure 2. BET proteins displayed conserved and masked mitotic activities

(A) Number of enriched mitotic GO terms and mitotic genes for the upregulated gene lists upon forced expression of various BET proteins in the OSK reprogramming cells.

(B) 31 mitotic GO terms enriched for the upregulated gene list upon overexpression of BRD2ΔBD1ΔET in the reprogramming cells. FE, fold enrichment; GO, gene ontology. Fisher Exact test; FDR, false discovery rate; FDR <0.05.

(C) Heatmaps for the 53 mitotic genes commonly upregulated by BETΔBD1ΔET (BRD2, BRD3, and BRD4S). The heatmaps were based on log2 (normalized read counts), scaled across the rows using the Pheatmap package.

(D) BET proteins have concealed mitotic activities in reprogramming cells as shown by cell cycle analyses with BRD4S as an example. ANOVA test, n = 3. *, $p < 0.05$. See also Figures S5–S7 and S12, and Tables S6 and S15.

Of note, 191 genes were commonly upregulated by the 3 BETΔBD1ΔET fragments (Figures S6C and S6F, Table S4); and 240 genes were commonly downregulated (Figures S6D and S6G, Table S5). Interestingly, both upregulation and downregulation were dose dependent (Figures S6E–S6G). Of the commonly upregulated genes, 64 displayed significantly higher expression levels in human embryonic stem cells (hESCs) than in the starting cells (Figure S6H), indicating legitimate up-reprogramming.[37] Of the commonly downregulated genes, 113 demonstrated enriched expression in fibroblasts (Figure S6I), representing the legitimate down-reprogramming.[37] In sum, the 3 BETΔBD1ΔET peptides commonly render 177 genes legitimate reprogramming.

BET peptides promote mitosis

We recently reported that BRD3R enhances reprogramming as well as mitosis in the early reprogramming cells.[19] GO analyses indicated that there was no enriched mitotic GO term for the upregulated gene lists in the reprogramming cells by the wild-type BET. In contrast, all the 3 upregulated gene lists by the 3 ΔBD1ΔET fragments resulted in many enriched mitotic GO terms (Figures 2A and 2B, and data not shown). A great number of genes were associated with the enriched mitotic GO terms in each of the 3 upregulated gene lists (Figure 2A). Critically, 53 of these mitotic genes were shared by the 3 BETΔBD1ΔET fragments (Figures 2C and S7A). The upregulation of these 53 mitotic genes was also proportional to the dosages of the BETΔBD1ΔET peptides (Figures 2C and S6E, Table S6). We also examined the mitosis activities of

the reprogramming cells at the cellular levels. Like their counterpart BRD3R, ET deletion from BRD2 also increased the mitotic cells, but not BRD4S (Figures 2D and S7B–S7D). Further deletion of BD1 or BD2 also increased mitotic cells for all three BET members, but double deletion of both bromodomains failed to increase the mitotic cells for BRD2 and BRD3. Unlike BRD2 and BRD3, ET deletion alone from BRD4S did not increase the mitotic cells but triple deletions in BRD4S increased mitotic activities (Figure 2D), indicating that masking of mitosis activity in BRD4S is tighter. Interestingly, as seen with BRD3R,[19] the mitosis activities for the BET deletion peptides generally correlated with their reprogramming activities.

BET regulate stress response in reprogramming cells

The BETΔBD1ΔET fragments predominantly downregulated genes (Figure S6B), and 240 genes are commonly downregulated by the three similar peptides of different BET proteins (BRD2ΔBD1ΔET, BRD3ΔBD1ΔET, and BRD4SΔBD1ΔET) (Figures S6D and S6G, Table S5). Given that these three deletion BETs displayed the most robust reprogramming activities (Figures 1B–1E), we conducted GO analyses for these 240 shared downregulated genes. Impressively, 131 out of the 240 genes were associated with the significantly enriched GO term of "response to stimulus" and 65 genes shared the enriched GO term of "response to stress" (Figure 3A) when only a total of 148 genes were associated with all the 47 GO terms significantly enriched (Figures 3A and 3B). In fact, other enriched GO terms were child GO terms of "response to stimulus" or "response to stress", or the related GO terms (Figures 3A and 3D). Only 10 genes were associated with non-stimulus/stress-response GO terms (Figures 3A and 3C). Literature mining indicated that some of the 10 genes may also have roles in stress responses but have not been curated so yet, for examples, *OBSL1*[39] and *PARP6*.[40] Of note, 54% of the downregulated stress-response genes have higher expression in the starting cells (Figure 3E), representing legitimate down-reprogramming.[37] In summary, almost all commonly downregulated genes in the reprogramming cells by the BET peptides that have an enriched GO term have a role in stress/stimulus responses.

BET regulate stress response in naive cells

We further explored whether our deletion mini-BETs also have impact on expression of the stress-response genes in the naive cells. To this end, we additionally sequenced RNA samples of human fibroblasts with forced expressions of the mini-BET proteins only (without the Yamanaka reprogramming factors). Many more genes are differentially expressed (DE) by the BETΔBD1ΔET fragments as compared to that in the reprogramming cells (Figures S8A–S8C, compared to S6B-D). As in the reprogramming cells, many more genes were downregulated than upregulated for all the three mini-BETs (Figure S8A). This agrees with the major roles of BET proteins in positive regulation of transcription when these mini-BET proteins are considered as dominant negative (see discussion). However, as in the reprograming cells, substantial number of genes was also upregulated (Figures S8A, S8C, and S8E). This is again not surprising considering that BET chemical inhibition in naive human fibroblasts also resulted in upregulation of a group of genes,[18] and that we observed similar patterns in the reprogramming cells. Impressively, 1,327 genes are commonly downregulated in naive fibroblasts by the 3 BETΔBD1ΔET fragments (Figures S8B and S8D, Table S7). Strikingly, GO analyses with these 1,327 genes showed that there were 128 significantly enriched stimulus/stress-response GO terms of various kinds (Figure 4A, Table S8). There should be more enriched stress-related GO terms since we did not include the keywords of "immune", "virus", "interferon", and others related to "stress responses". Of these, 341 genes were associated with the single enriched GO term of "response to stress" (Figure 4A, and Table S8). In total, 734 genes (55.3%) were in the general category of stress/stimulus responses (Figure 4B, Table S9). In summary, our data indicate that the 3 human BET proteins regulate stimulus/stress responses even in the naive cells (non-reprogramming cells).

We further explored whether any bromodomain is required for the downregulation of stress-response genes. To this end, we additionally conducted RNA-seq on human fibroblasts overexpressing BRD3RΔBD2 or BRD3RΔBD1ΔBD2. Strikingly, 714 genes are commonly downregulated by all 5 mini-BETs (BRD3RΔBD1, BRD3RΔBD2, BRD3RΔBD1ΔBD2, BRD2ΔBD1ΔET, and BRD4SΔBD1ΔET) (Figure 5A). GO analyses of these 714 common genes again revealed that 434 genes, which are associated with any enriched GO term, have roles in stress/stimulus responses (Figures 5B and 5C). These combined results indicate that the conserved targeting of the stress/stimulus-response genes by the BET peptides is independent of the three characteristic domains (2 BD and the ET domains). This conclusion applies at least to BRD3 for which we sequenced RNA samples for all BRD3 deletion conditions.

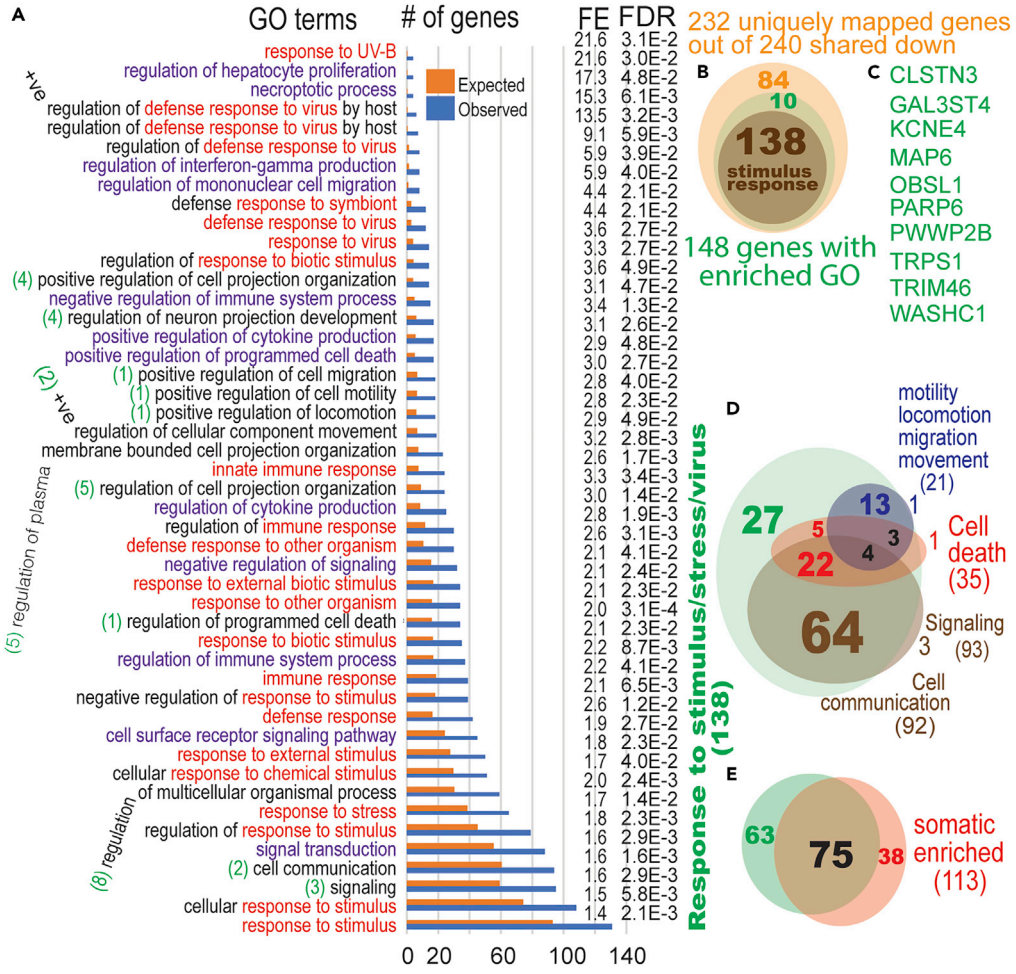

Figure 3. Almost all commonly downregulated genes by BETΔBD1ΔET with enriched GO terms have roles in stress/stimulus responses

(A) The full list of significantly enriched GO terms for the 240 genes commonly downregulated by the BETΔBD1ΔET fragments. Red, stress/stimulus-response GO terms; purple, GO terms for which all the genes have explicit stress/stimulus GO terms as well; numbers in brackets before GO terms are number of genes in the GO term that are not among the 138 genes with enriched stress/stimulus-response GO terms. FE, fold enrichment; GO, gene ontology. Fisher Exact test; FDR, false discovery rate; FDR <0.05.

(B and C) Venn diagram (B) showing only 10 of the genes with enriched GO terms does not have annotated stimulus/stress-response GO terms, and the name of these 10 genes (C).

(D) Other non-stress-response GO terms in A mainly contain stress/stimulus-response genes with related or other roles.

(E) 54% of the 138 downregulated stimulus/stress-response genes represent legitimate down reprogramming.See also Figure S6 and Table S5.

BET peptides and chemical inhibitors commonly target stress-response genes

We previously reported that mild chemical targeting of BET proteins also promoted human iPSC reprogramming.[18] When compared with the 5 BET deletion fragments described above, JQ1 commonly downregulated 141 genes. These 141 genes have 5 enriched GO terms only, and all are in the category of stimulus/stress response (Figure 5D). There were 85 stress-response genes in these 5 enriched GO terms (60.3% of the 141 genes). In conclusion, the BET chemical inhibitors and the 5 BET peptides target a common set of stress-response genes.

BET peptides upregulate chemical responses

We noticed that the BETΔBD1ΔET fragments also upregulated many more genes in naive fibroblasts than in reprogramming fibroblasts (compare Figures S8A, S8C, and S8E with S6B, S6C, and S6F). Out of these

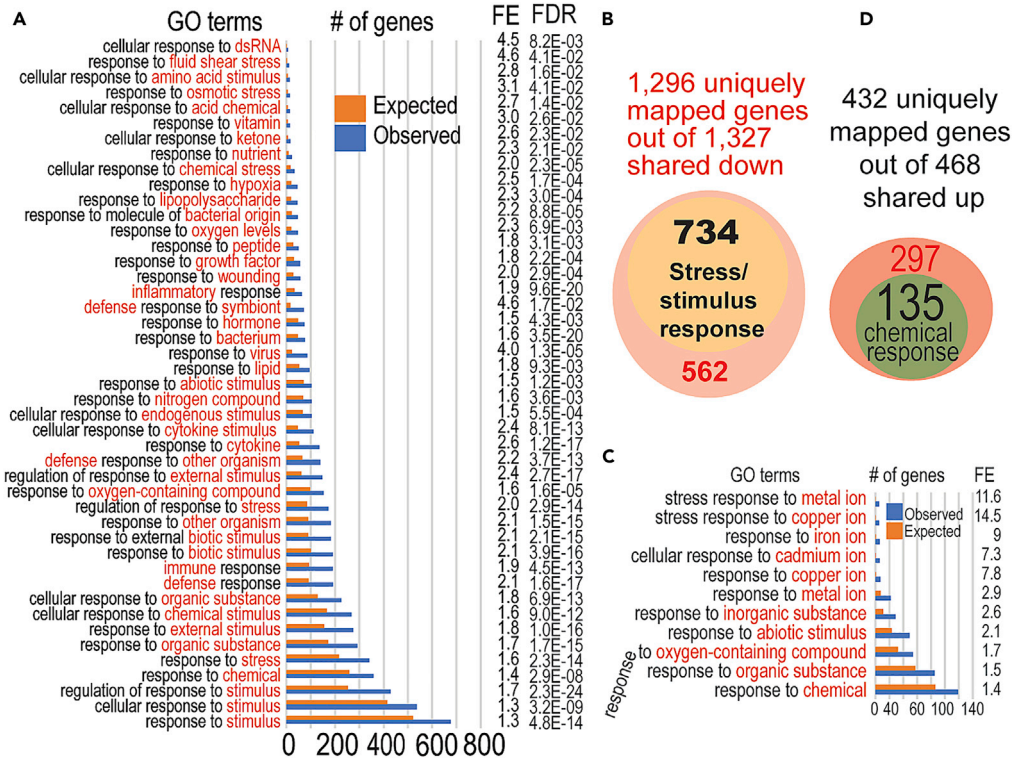

Figure 4. The DN BETΔBD1ΔET fragments predominantly suppress transcription of stress/stimulus-response genes of various categories in naive human fibroblasts

(A) 47 selected enriched stimulus/stress-response GO terms with the most gene numbers or representative response categories among the significantly enriched GO terms of the 1,336 shared downregulated genes. The stimulant categories are highlighted in red in the GO terms. FE, fold enrichment; GO, gene ontology. Fisher Exact test; FDR, false discovery rate; FDR <0.05.

(B) 56.6% (734 genes) of the mapped genes (1,296 genes) have stress/stimulus-response GO terms of a wide range of categories for the commonly downregulated genes in human fibroblasts.

(C) Complete list of enriched stimulus/stress-response GO terms showing exclusive chemical response categories for the upregulated genes by the BETΔBD1ΔET fragments in naive human fibroblasts.

(D) Skewed upregulation of chemical response genes by the BETΔBD1ΔET fragments in human fibroblasts.

upregulated genes, 468 were shared by the three BET fragments indicating a common mechanism among BRD2, BRD3, and BRD4 (Figures S8C and S8E). Of note, 119 of the upregulated genes were associated with the single GO term of "response to chemical", and 135 upregulated genes were in this category if all the 11 enriched chemical-response GO terms were considered (Figures 4C and 4D). Some GO terms such as "detoxification of copper ion" do not contain the keywords used in our original inquiry. When these are also included, the extended "chemical response" includes 155 genes. Compared to that of the downregulated genes, there are two major differences in terms of enrichment of the stress-response GO terms. First, much smaller portion of genes are in the stress-response category (33.2% vs 66.1%); second, the upregulated genes are exclusively in the "chemical response" category, but the downregulated genes represent a wide range of various stress/stimulus responses. Interestingly, at least some of these upregulated genes may have roles in detoxification of chemicals, indicating a positive role in cell biology for these upregulated genes in stress responses.

BET deletion peptides mitigate the observed reprograming stress

Given the predominant stress-response GO terms enriched in the commonly downregulated genes by the BETΔBD1ΔET fragments that displayed the highest reprogramming activities, we started to evaluate reprogramming stress and asked whether the BETΔBD1ΔET fragments mitigate reprogramming stress if any. Impressively, 5,083 genes were significantly disrupted transcriptionally by OSKM (Figure S9A), representing 40.5% of all transcribed genes of human fibroblasts (Figure 6A). Without the pro-oncogene MYC,

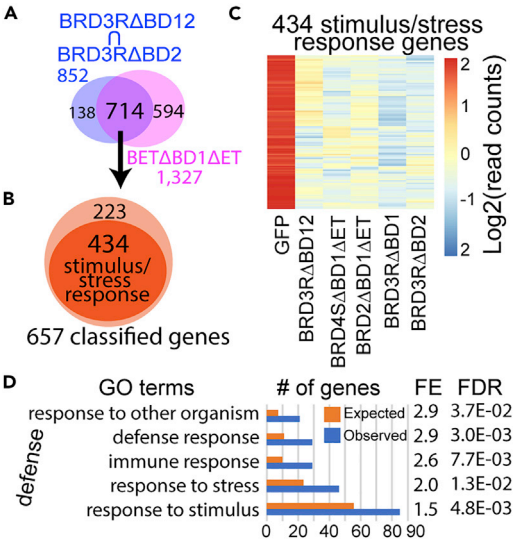

Figure 5. The bromodomain-null DN BET fragments and chemical targeting of bromodomains commonly downregulate stress/stimulus-response genes

(A) BET deletion fragments devoid of individual or both bromodomains commonly downregulated 741 genes.

(B) The commonly downregulated genes predominantly have functions of stress/stimulus responses.

(C) Heatmaps for the 434 stress/stimulus-response genes downregulated commonly by all the 5 BET deletion mutants in human fibroblasts. Heatmaps were based on averaged normalized read counts in the log2 scale. GFP, n = 3; all mutant RNA-seq, n = 2 except for BRD3RΔBD12, for which n = 3.

(D) Complete list of enriched GO terms for the 141 genes commonly downregulated genes in human reprogramming cells by BET chemical inhibitors and BET DN fragments.

OSK still deregulated 4,025 genes (Figure S9A), representing 32% of the fibroblast transcriptome (Figure 6A). In contrast, the transcription disruption by the wild-type BET proteins was low (1,184, 40, and 1,587 genes for BRD2, BRD3, and BRD4S, respectively). This global deregulation of transcription represents dramatic disruption to the transcription program of the starting cells, and we call it transcriptional turbulence given the scale of deregulation.

The BETΔBD1ΔET fragments also caused transcription changes to fibroblasts but to less degrees as compared to the reprogramming factors (Figure S9A). All 3 BETΔBD1ΔET fragments significantly downregulated transcription more than upregulation (Figure S9A). Unlike the BETΔBD1ΔET fragments, the reprogramming factors almost equally down- and upregulated transcription (for both OSK and OSKM) (Figure S9A), indicating a more random disruption of transcription as compared to the biased downregulation by the BETΔBD1ΔET fragments. We recently developed a method to measure global transcriptional differences.[35] Quantification of global transcriptional turbulence using our published method[35] also indicated that the Yamanaka factors caused great transcriptional turbulence with the wild-type BET as references (Figure 6B).

Given the predominant enrichment for the stress-response GO terms described above, we next tallied the stress/stimulus-response genes. We focused on the OSK reprogramming condition excluding MYC since it is a strong oncogene eliciting oncogene stress when overexpressed.[17] Upon forced expression of OSK, a large number of DE genes are represented by the enriched GO terms of stimulus/stress responses for both the up- (Tables 11 and S13, Figure S9F) and the downregulated (Tables 12 and S14, Figure S9G) genes by OSK as compared to GFP control, representing 44.7% and 43.7% of the down- and upregulated genes (Figure S9B). Of note, while OSK elicit dramatic expression changes for stress/stimulus-response genes, the fractions of stress/stimulus genes are almost the same for the down- and upregulated genes in the OSK reprogramming cells (Figure S9B). On the other hand, the stress/stimulus-response genes accounted for 57.5% of the downregulated genes, but only 19.2% for the upregulated genes by the BETΔBD1ΔET fragments (Figure S9B). In addition, only 3 stimulus/stress-response GO terms were marginally enriched for the upregulated gene list by the BETΔBD1ΔET fragments. Further scrutiny of the BETΔBD1ΔET upregulated genes indicates that 17 of the 54 stimulus/stress-response genes were associated with mitotic GO terms as well, indicating that the upregulated stress-response genes by the BETΔBD1ΔET fragments have positive roles in cell proliferation/survival. In naive human fibroblasts, the BETΔBD1ΔET fragments also predominantly downregulated stress-response genes. To sum, OSK randomly dysregulate a large set of stress-response genes while BETΔBD1ΔET fragments almost exclusively downregulated stress-response genes and many of the upregulated stress-response genes may represent a positive (survival) response to stress. In other words, OSK result in but BETΔBD1ΔET fragments attenuate reprograming stress based on their different patterns of dysregulation of the stress-response genes.

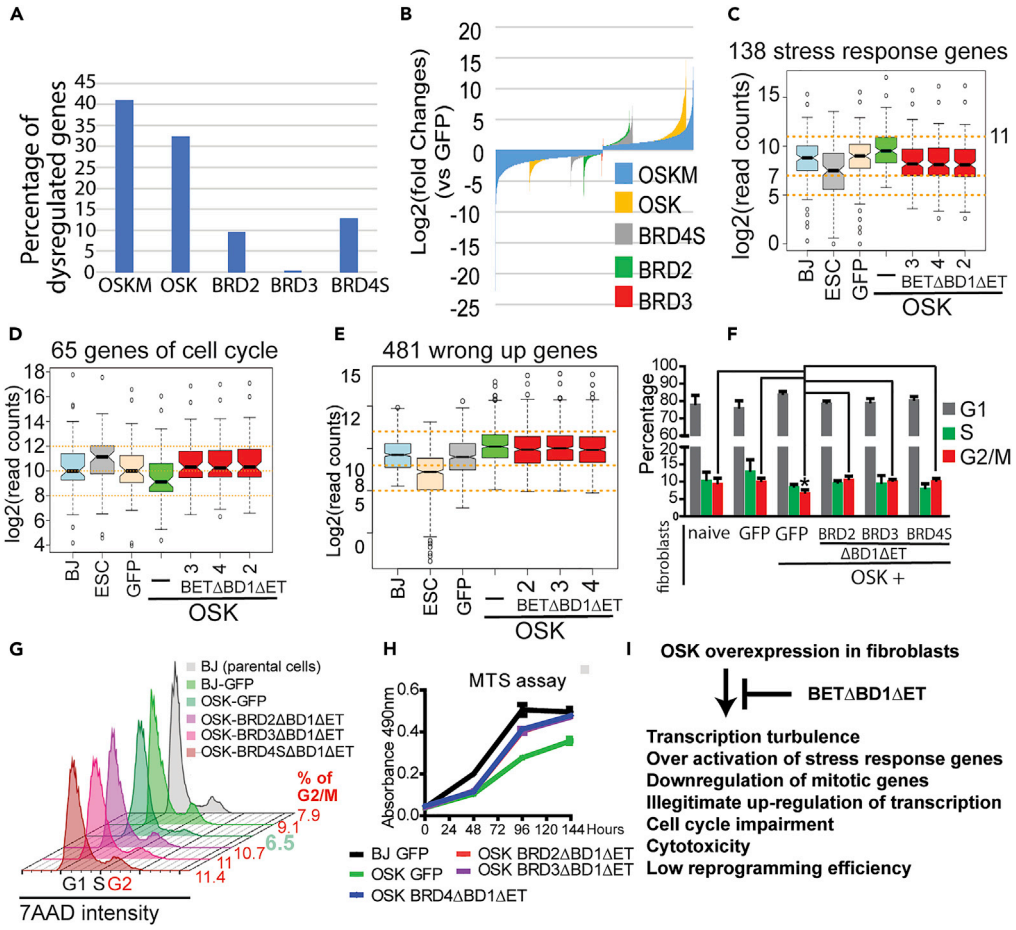

Figure 6. The BETΔBD1ΔET fragments mitigate reprogramming stresses

(A) Percentage of deregulated gene numbers relative to total expressed genes in the starting cells by overexpression of Yamanaka factors. The epigenetic readers BRD2, BRD3, and BRD4S are used references. The results are based on RNA-seq data. Differentially expressed genes are defined at $q < 0.05$ and 1.5-fold change levels.

(B) Waterfall plots demonstrating the total amount of transcriptional changes by Yamanaka reprogramming factors as measured by cumulative log2(fold changes).

(C) 138 stress-response genes are overactivated by OSK but mitigated by the BETΔBD1ΔET mutants in the reprogramming cells. Boxplots in a, b, and c are based on averaged normalized RNA-seq read counts in log2 scale. BJ, n = 8; ESC, n = 7; GFP, n = 3; OSK, n = 3; all BET mutant RNA-seq, n = 2.

(D) 65 cell cycle genes are compromised by the reprogramming factors but mitigated by BETΔBD1ΔET fragment in the reprogramming cells.

(E) A group of 481 genes were wrongly up-reprogrammed and mitigated by the BETΔBD1ΔET fragments albeit to a lesser extent.

(F) Cell cycle profiling by flow cytometry showing compromised cell cycle profiles by OSK reprogramming factors, but mitigated by various BET deletion fragments in the early reprogramming cells. Unpaired, two-sided T test, n = 3. *, $p < 0.05$.

(G) Representative histogram of cell cycle profiles determined by flow cytometry, showing compromised G2/M population but attenuated by the BET deletion mutants in the OSK reprogramming cells.

(H) Reprogramming factors results in cytotoxicity but mitigated by BETΔBD1ΔET in the reprogramming cells. The same number of cells was seeded at 0 h from cells at 24 h post transduction. The means ± SEM were plotted. n = 3.

(I) Summary for attenuation of reprogramming stresses by the dominant-negative BETΔBD1ΔET fragments. See also Figure S9, and Tables S6, S10, S11, S13, and S14.

Next, we analyzed the 138 stress-response genes commonly downregulated by the BETΔBD1ΔET fragments in the reprogramming cells (Figures 3 B, 3D, 3E, Table S10). GFP had little impact on these 138 genes (Figure 6C), but they were upregulated significantly by OSK as compared to the naive and GFP controls, implying a strong stress response to the reprogramming factors. Such transcriptional upregulation was

removed by all 3 BETΔBD1ΔET fragments in the reprogramming cells (Figure 6C). Furthermore, these 138 genes have much lower expression in hESCs (Figure 6C), indicating legitimate down-reprogramming by the BETΔBD1ΔET fragments in addition to stress release.

Cell cycles are generally impacted under stress.[41] Given that the BETΔBD1ΔET fragments commonly up-regulated 53 mitotic genes, we further compared the 64 cell cycles genes (including the 53 mitotic genes) commonly upregulated by the 3 BETΔBD1ΔET fragments in the OSK reprogramming cells (Table S6). Their expression was indeed compromised by OSK as compared to the naive and GFP controls, further indicating a reprogramming stress (Figure 6D, Table S6). Again, all 3 BETΔBD1ΔET fragments attenuated the impairment in cell cycle gene expression (Figure 6D).

We asked whether the BETΔBD1ΔET fragments mitigate the aberrant up-reprogramming by OSK as we reported before.[37] Indeed, the 3 BETΔBD1ΔET fragments attenuated the wrong up-reprogramming although the expression levels were not restored to the state of the starting cells (Figure 6E).

After demonstrating the mitigation of reprogramming stress at the molecular levels, we further tested whether OSK compromise the reprogramming cells at the cellular levels and whether the BETΔBD1ΔET fragments could mitigate it if any. At the cellular levels, flow cytometry showed that OSK reduced the population of G2/M cells (to 6.5% in Figure 6G) and the BETΔBD1ΔET fragments increased the G2/M population to the levels even slightly higher than that in the starting naive cells and GFP controls (Figures 6F and 6G). OSK resulted in cytotoxicity and the BETΔBD1ΔET fragments have mitigated such a negative impact on the reprogramming cells by OSK (Figure 6H). In agreement with our previous observation with BRD3R,[19] the 3 BETΔBD1ΔET fragments interestingly did not affect apoptosis in reprogramming cells as evaluated by different methods including annexin V, caspase 8 activity, and TUNEL assay (Figures S9C–S9E).

DISCUSSION

To understand the underlying mechanisms for the observed reprogramming activity of BRD3R (the short isoform of human BRD3),[19] this study generated a series of deletion proteins of human BRD2, BRD3, and BRD4. Several lines of evidence indicate that these BET fragments are dominant negative, especially for the BETΔBD1ΔET fragments. First, they all displayed reprogramming activities as do the BET chemical inhibitors.[18] Second, these peptides predominantly downregulated genes in agreement with the BET roles as positive regulators of transcription, and such downregulation are consistent between reprogramming and naive cells. Third, the downregulated genes by these BET peptides largely overlap that by the BET chemical inhibitors. Fourth, the above three phenomena are conserved among the 3 similar peptides of the 3 ubiquitous human BET proteins, BRD2, BRD3, and BRD4.

The critical finding, as a byproduct of our reprograming study, is that both these BET peptides and the BET chemical inhibitors commonly downregulated a large set of stress-response genes. In fact, the only enriched GO category for the commonly downregulated genes by the BET chemical inhibitors and the BETΔBD1ΔET peptides in the reprogramming cells is stress response. Of note, this is true for the extreme deletion that lacks the ET tails and both bromodomains. Of note, the upregulation of a set of mitotic genes by the DN BET proteins is consistent with their roles in regulation of stress responses because mitotic and cell cycle genes are usually compromised by cellular stresses. BET regulation of stress-response genes including mitotic genes reported here is very reliable because we consistently observed such a phenomenon from RNA-seq data of all three BET members. RNA-seq is very sensitive and reliable based on our experiences of many years.[42] Our NanoString data on these stress-response mitotic gene sets were highly consistent with the RNA-seq data (see Figure S12, and Table S15). The chemical inhibitors target the bromodomains, but our BET peptides are lacking the bromodomains. Therefore, our peptide targeting of BET proteins may represent a unique unreported targeting mechanism. The peptide targeting of BET functions may provide a novel approach to managing the BET-associated diseases. These DN BET deletion fragments will also be invaluable research tools in BET biology.

The Yamanaka reprogramming is stochastic and inefficient, but the underlying molecular causes remain elusive. This study provides evidence for the concept of reprogramming stress. First, the Yamanaka factors elicit dramatic transcriptional turbulence to the starting cells. Second, even without the oncogene MYC,

OSK predominantly dysregulate stress-response genes, and such responses seem stochastic considering that there were similar degrees of up- and downregulation of stimulus-response genes. Third, OSK molecularly compromise mitotic genes. Fourth, OSK impair cell cycle of the starting cells. Fifth, OSK cause cytotoxicity to the starting cells. Interestingly, all these reprogramming stresses are mitigated by our BETΔBD1ΔET peptides. Furthermore, the BETΔBD1ΔET peptides additionally mitigate the aberrant reprogramming for the wrongly up-reprogrammed genes. However, we failed to observe impact on apoptosis of the reprogramming populations by the BETΔBD1ΔET peptides. Reprogramming-associated specialized stresses have been reported before,[7–15,43] but our current data indicate that the BETΔBD1ΔET peptides mitigate a more general reprogramming stress. It is well known that oncogenes can elicit cellular stresses.[16,17] Literature indicates that all reprogramming factors play a role in cancers.[44–46] In the future, it will be interesting to explore if any one or two of the three (OSK) are able to elicit the reprogramming stress we observed here. However, it should be stressed that OSK is the minimum combination of reprogramming factors to convert human fibroblasts to iPSCs.

We proposed that the BETΔBD1ΔET fragments enhance reprogramming by attenuating various reprogramming stresses caused by OSK as summarized in Figure 6I. However, the BETΔBD1ΔET fragments may promote reprogramming through multiple mechanisms including enhancing mitosis activity[19] and silencing and/or downregulation of the somatic genes as proposed before.[18,30] Although Gurdon's and Eggan's groups demonstrated that mitosis plays critical roles in reprogramming using the traditional nuclear transfer method,[47,48] we now more favor the stress release model for the increased reprogramming regarding enhancement of mitosis in the reprogramming cells by our BET deletion proteins given that cell cycle impairment is a hallmark of cellular stress and other data reported here.

Limitations of the study

Fibroblasts are the most common starting cells for iPSC reprogramming. All observations here are based on research using human fibroblasts. However, other somatic cells such as keratinocytes and various blood cells can be converted into iPSCs. In the future, it is worth to explore whether what were observed in fibroblast reprogramming apply to other starting cells of reprogramming.

We have made extensive deletion of BET proteins and showed that these deletion mini-BET enhance reprogramming and mitosis, as well as mitigate various types of reprogramming stress. It is necessary to define the minimum sequences and sequence determinants for the observed activities seen in our mini-BET fragments. Our laboratory is making such an effort since this may help establish a different mechanism of BET inhibition. We also do not know how the mini-BET fragments target their parent proteins, and this will be a major effort of our future investigation.

In this study, we demonstrated that our mini-BET proteins mitigate reprogramming stress at both molecular and cellular levels. We used two cellular readouts, impaired cell cycles and cytotoxicity, which are the two hallmarks of cellular stress. Literature indicates that iPSC reprogramming causes various cellular stresses including oxidative stress, ER stress, and replication stress. We have not tested whether our mini-BET proteins can mitigate these stresses in the reprogramming cells, and this constitutes a future direction of research.

STAR★METHODS

Detailed methods are provided in the online version of this paper and include the following:

- KEY RESOURCES TABLE
- RESOURCE AVAILABILITY
  - Lead contact
  - Materials availability
  - Data and code availability
- EXPERIMENTAL MODEL AND SUBJECT DETAILS
  - Human fibroblast cells
- METHOD DETAILS
  - Cell culture
  - Plasmids

- Plasmid preparation for virus packaging
- Virus packaging
- Virus concentration
- Titration of lentiviral particles
- Cell culture and reprogramming
- Reprogramming with Sendai vectors
- Alkaline phosphatase (ALP) staining
- TRA1-60 staining of iPSC colonies
- Immunocytochemistry and microscopy
- Detection of pluripotency surface markers by flow cytometry
- TUNNEL assay
- Caspase 8 activity assay
- Annexin V staining
- Cell cycle analyses
- Cell viability and cytotoxicity assay
- Teratoma assays
- Karyotyping
- RNA preparation for RNA-seq
- RNA-seq
- Bioinformatics
- Quantitate transcriptional turbulence caused by the yamanaka factors
- NanoString nCounter^{TM} quantification of gene expression

- QUANTIFICATION AND STATISTICAL ANALYSES

SUPPLEMENTAL INFORMATION

Supplemental information can be found online at https://doi.org/10.1016/j.isci.2022.105889.

ACKNOWLEDGMENTS

This work was supported by a fund from National Institutes of Health (NIH) (R01GM127411) to K.H. We appreciate the infrastructure and staff support from UAB Comprehensive Flow Cytometry Core, the UAB Research Computing unit, UAB Comparative Pathology Laboratory, and UAB Animal Resources Program. We thank Novogene and Genewiz for their sequencing services, and Cell Line Genetics (Madison, Wisconsin) for karyotyping. We thank Drs. Tim Townes and Kevin Pawlik for their fluorescence microscope. We thank Dr. Louise Chow for critical reading of this manuscript before submission. We thank Dr. Jianqing Zhang from UAB NanoString Laboratory for his technical help in nCounter analyses.

AUTHOR CONTRIBUTIONS

Conceptualization, K.H.; Methodology, K.H., M.E.H., R.R.C., R.Z.; Investigation, K.H., M.E.H., R.R.C., R.Z.; Validation, K.H., M.E.H., R.R.C., R.Z.; Formal Analysis, K.H., M.E.H., R.R.C.; Writing – Original Draft, K.H.; Writing – Review and Editing, K.H., M.E.H., R.R.C., R.Z.; Resources, K.H.; Data Curation, K.H., R.R.C.; Visualization, K.H., R.R.C.; Supervision, K.H.; Funding Acquisition, K.H.

DECLARATION OF INTERESTS

All authors declare no competing interests.

INCLUSION AND DIVERSITY

One or more of the authors of this paper self-identifies as an underrepresented ethnic minority in their field of research or within their geographical location. We support inclusive, diverse, and equitable conduct of research.

Received: July 26, 2022
Revised: November 6, 2022
Accepted: December 23, 2022
Published: January 20, 2023

REFERENCES

1. Takahashi, K., Okita, K., Nakagawa, M., and Yamanaka, S. (2007). Induction of pluripotent stem cells from fibroblast cultures. Nat. Protoc. *2*, 3081–3089. https://doi.org/10.1038/nprot.2007.418.

2. Takahashi, K., and Yamanaka, S. (2006). Induction of pluripotent stem cells from mouse embryonic and adult fibroblast cultures by defined factors. Cell *126*, 663–676. https://doi.org/10.1016/j.cell.2006.07.024.

3. Hu, K. (2014). All roads lead to induced pluripotent stem cells: the technologies of iPSC generation. Stem Cell. Dev. *23*, 1285–1300. https://doi.org/10.1089/scd.2013.0620.

4. Deng, W., Jacobson, E.C., Collier, A.J., and Plath, K. (2021). The transcription factor code in iPSC reprogramming. Curr. Opin. Genet. Dev. *70*, 89–96. https://doi.org/10.1016/j.gde.2021.06.003.

5. Hu, K. (2014). Vectorology and factor delivery in induced pluripotent stem cell reprogramming. Stem Cell. Dev. *23*, 1301–1315. https://doi.org/10.1089/scd.2013.0621.

6. Haridhasapavalan, K.K., Raina, K., Dey, C., Adhikari, P., and Thummer, R.P. (2020). An insight into reprogramming barriers to iPSC generation. Stem Cell Rev. Rep. *16*, 56–81. https://doi.org/10.1007/s12015-019-09931-1.

7. Qi, S., Fang, Z., Wang, D., Menendez, P., Yao, K., and Ji, J. (2015). Concise review: induced pluripotency by defined factors: prey of oxidative stress. Stem Cell. *33*, 1371–1376. https://doi.org/10.1002/stem.1946.

8. Simic, M.S., Moehle, E.A., Schinzel, R.T., Lorbeer, F.K., Halloran, J.J., Heydari, K., Sanchez, M., Jullié, D., Hockemeyer, D., and Dillin, A. (2019). Transient activation of the UPR(ER) is an essential step in the acquisition of pluripotency during reprogramming. Sci. Adv. *5*, eaaw0025. https://doi.org/10.1126/sciadv.aaw0025.

9. Ruiz, S., Lopez-Contreras, A.J., Gabut, M., Marion, R.M., Gutierrez-Martinez, P., Bua, S., Ramirez, O., Olalde, I., Rodrigo-Perez, S., Li, H., et al. (2015). Limiting replication stress during somatic cell reprogramming reduces genomic instability in induced pluripotent stem cells. Nat. Commun. *6*, 8036. https://doi.org/10.1038/ncomms9036.

10. Guallar, D., Fuentes-Iglesias, A., Souto, Y., Ameneiro, C., Freire-Agulleiro, O., Pardavila, J.A., Escudero, A., Garcia-Outeiral, V., Moreira, T., Saenz, C., et al. (2020). ADAR1-Dependent RNA editing promotes MET and iPSC reprogramming by alleviating ER stress. Cell Stem Cell *27*, 300–314.e11. https://doi.org/10.1016/j.stem.2020.04.016.

11. Chiou, S.S., Wang, S.S.W., Wu, D.C., Lin, Y.C., Kao, L.P., Kuo, K.K., Wu, C.C., Chai, C.Y., Lin, C.L.S., Lee, C.Y., et al. (2013). Control of oxidative stress and generation of induced pluripotent stem cell-like cells by jun dimerization protein 2. Cancers *5*, 959–984. https://doi.org/10.3390/cancers5030959.

12. Xu, X., Wang, Q., Long, Y., Zhang, R., Wei, X., Xing, M., Gu, H., and Xie, X. (2013). Stress-mediated p38 activation promotes somatic cell reprogramming. Cell Res. *23*, 131–141. https://doi.org/10.1038/cr.2012.143.

13. Banito, A., Rashid, S.T., Acosta, J.C., Li, S., Pereira, C.F., Geti, I., Pinho, S., Silva, J.C., Azuara, V., Walsh, M., et al. (2009). Senescence impairs successful reprogramming to pluripotent stem cells. Genes Dev. *23*, 2134–2139. https://doi.org/10.1101/gad.1811609.

14. Marión, R.M., Strati, K., Li, H., Murga, M., Blanco, R., Ortega, S., Fernandez-Capetillo, O., Serrano, M., and Blasco, M.A. (2009). A p53-mediated DNA damage response limits reprogramming to ensure iPS cell genomic integrity. Nature *460*, 1149–1153. https://doi.org/10.1038/nature08287.

15. Hong, H., Takahashi, K., Ichisaka, T., Aoi, T., Kanagawa, O., Nakagawa, M., Okita, K., and Yamanaka, S. (2009). Suppression of induced pluripotent stem cell generation by the p53-p21 pathway. Nature *460*, 1132–1135. https://doi.org/10.1038/nature08235.

16. Curti, L., and Campaner, S. (2021). MYC-induced replicative stress: a double-edged sword for cancer development and treatment. Int. J. Mol. Sci. *22*, 6168. https://doi.org/10.3390/ijms22126168.

17. Haigis, K.M., and Sweet-Cordero, A. (2011). New insights into oncogenic stress. Nat. Genet. *43*, 177–178. https://doi.org/10.1038/ng0311-177.

18. Shao, Z., Yao, C., Khodadadi-Jamayran, A., Xu, W., Townes, T.M., Crowley, M.R., and Hu, K. (2016). Reprogramming by de-bookmarking the somatic transcriptional program through targeting of BET bromodomains. Cell Rep. *16*, 3138–3145. https://doi.org/10.1016/j.celrep.2016.08.060.

19. Shao, Z., Zhang, R., Khodadadi-Jamayran, A., Chen, B., Crowley, M.R., Festok, M.A., Crossman, D.K., Townes, T.M., and Hu, K. (2016). The acetyllysine reader BRD3R promotes human nuclear reprogramming and regulates mitosis. Nat. Commun. *7*, 10869. https://doi.org/10.1038/ncomms10869.

20. Nakagawa, M., Koyanagi, M., Tanabe, K., Takahashi, K., Ichisaka, T., Aoi, T., Okita, K., Mochiduki, Y., Takizawa, N., and Yamanaka, S. (2008). Generation of induced pluripotent stem cells without Myc from mouse and human fibroblasts. Nat. Biotechnol. *26*, 101–106. https://doi.org/10.1038/nbt1374.

21. Cheung, K.L., Kim, C., and Zhou, M.M. (2021). The functions of BET proteins in gene transcription of biology and diseases. Front. Mol. Biosci. *8*, 728777. https://doi.org/10.3389/fmolb.2021.728777.

22. Ali, H.A., Li, Y., Bilal, A.H.M., Qin, T., Yuan, Z., and Zhao, W. (2022). A comprehensive review of BET protein biochemistry, physiology, and pathological roles. Front. Pharmacol. *13*, 818891. https://doi.org/10.3389/fphar.2022.818891.

23. Michaeloudes, C., Mercado, N., Clarke, C., Bhavsar, P.K., Adcock, I.M., Barnes, P.J., and Chung, K.F. (2014). Bromodomain and extraterminal proteins suppress NF-E2-related factor 2-mediated antioxidant gene expression. J. Immunol. *192*, 4913–4920. https://doi.org/10.4049/jimmunol.1301984.

24. Zhang, J., Dulak, A.M., Hattersley, M.M., Willis, B.S., Nikkilä, J., Wang, A., Lau, A., Reimer, C., Zinda, M., Fawell, S.E., et al. (2018). BRD4 facilitates replication stress-induced DNA damage response. Oncogene *37*, 3763–3777. https://doi.org/10.1038/s41388-018-0194-3.

25. Segatto, M., Szokoll, R., Fittipaldi, R., Bottino, C., Nevi, L., Mamchaoui, K., Filippakopoulos, P., and Caretti, G. (2020). BETs inhibition attenuates oxidative stress and preserves muscle integrity in Duchenne muscular dystrophy. Nat. Commun. *11*, 6108. https://doi.org/10.1038/s41467-020-19839-x.

26. Hussong, M., Börno, S.T., Kerick, M., Wunderlich, A., Franz, A., Sültmann, H., Timmermann, B., Lehrach, H., Hirsch-Kauffmann, M., and Schweiger, M.R. (2014). The bromodomain protein BRD4 regulates the KEAP1/NRF2-dependent oxidative stress response. Cell Death Dis. *5*, e1195. https://doi.org/10.1038/cddis.2014.157.

27. Wang, N., Wu, R., Tang, D., and Kang, R. (2021). The BET family in immunity and disease. Signal Transduct. Targeted Ther. *6*, 23. https://doi.org/10.1038/s41392-020-00384-4.

28. Nicodeme, E., Jeffrey, K.L., Schaefer, U., Beinke, S., Dewell, S., Chung, C.W., Chandwani, R., Marazzi, I., Wilson, P., Coste, H., et al. (2010). Suppression of inflammation by a synthetic histone mimic. Nature *468*, 1119–1123. https://doi.org/10.1038/nature09589.

29. Liu, L., Xu, Y., He, M., Zhang, M., Cui, F., Lu, L., Yao, M., Tian, W., Benda, C., Zhuang, Q., et al. (2014). Transcriptional pause release is a rate-limiting step for somatic cell reprogramming. Cell Stem Cell *15*, 574–588. https://doi.org/10.1016/j.stem.2014.09.018.

30. Li, X., Zuo, X., Jing, J., Ma, Y., Wang, J., Liu, D., Zhu, J., Du, X., Xiong, L., Du, Y., et al. (2015). Small-molecule-driven direct reprogramming of mouse fibroblasts into functional neurons. Cell Stem Cell *17*, 195–203. https://doi.org/10.1016/j.stem.2015.06.003.

31. Hnilicová, J., Hozeifi, S., Stejskalová, E., Dušková, E., Poser, I., Humpolíčková, J., Hof, M., and Staněk, D. (2013). The C-terminal domain of Brd2 is important for chromatin interaction and regulation of transcription and alternative splicing. Mol. Biol. Cell *24*, 3557–3568. https://doi.org/10.1091/mbc.E13-06-0303.

32. Filippakopoulos, P., Qi, J., Picaud, S., Shen, Y., Smith, W.B., Fedorov, O., Morse, E.M., Keates, T., Hickman, T.T., Felletar, I., et al. (2010). Selective inhibition of BET bromodomains. Nature *468*, 1067–1073. https://doi.org/10.1038/nature09504.

33. Shao, Z., Cevallos, R.R., and Hu, K. (2021). Reprogramming human fibroblasts to induced pluripotent stem cells using the GFP-marked lentiviral vectors in the chemically defined medium. Methods Mol. Biol. *2239*, 101–116. https://doi.org/10.1007/978-1-0716-1084-8_7.

34. Kang, L., Yao, C., Khodadadi-Jamayran, A., Xu, W., Zhang, R., Banerjee, N.S., Chang, C.W., Chow, L.T., Townes, T., and Hu, K. (2016). The universal 3D3 antibody of human PODXL is pluripotent cytotoxic, and identifies a residual population after extended differentiation of pluripotent stem cells. Stem Cell. Dev. *25*, 556–568. https://doi.org/10.1089/scd.2015.0321.

35. Hu, K., Ianov, L., and Crossman, D. (2020). Profiling and quantification of pluripotency reprogramming reveal that WNT pathways and cell morphology have to be reprogramed extensively. Heliyon *6*, e04035. https://doi.org/10.1016/j.heliyon.2020.e04035.

36. Hu, K. (2020). Quick, coordinated and authentic reprogramming of ribosome biogenesis during iPSC reprogramming. Cells *9*, 2484. https://doi.org/10.3390/cells9112484.

37. Hu, K. (2020). A PIANO (proper, insufficient, aberrant, and NO reprogramming) response to the Yamanaka factors in the initial stages of human iPSC reprogramming. Int. J. Mol. Sci. *21*, 3229. https://doi.org/10.3390/ijms21093229.

38. Cevallos, R.R., Edwards, Y.J.K., Parant, J.M., Yoder, B.K., and Hu, K. (2020). Human transcription factors responsive to initial reprogramming predominantly undergo legitimate reprogramming during fibroblast conversion to iPSCs. Sci. Rep. *10*, 19710. https://doi.org/10.1038/s41598-020-76705-y.

39. Hiebel, C., Sturner, E., Hoffmeister, M., Tascher, G., Schwarz, M., Nagel, H., Behrends, C., Munch, C., and Behl, C. (2020). BAG3 proteomic signature under proteostasis stress. Cells *9*, 2416. https://doi.org/10.3390/cells9112416.

40. Ke, Y., Wang, C., Zhang, J., Zhong, X., Wang, R., Zeng, X., and Ba, X. (2019). The role of PARPs in inflammation-and metabolic-related diseases: molecular mechanisms and beyond. Cells *8*, 1047. https://doi.org/10.3390/cells8091047.

41. Fulda, S., Gorman, A.M., Hori, O., and Samali, A. (2010). Cellular stress responses: cell survival and cell death. Int. J. Cell Biol. *2010*, 214074. https://doi.org/10.1155/2010/214074.

42. Hu, K. (2022). RNA-seq Analyses Using HPC: A Tutorial for Bench Scientists (Bookbaby).

43. Kawamura, T., Suzuki, J., Wang, Y.V., Menendez, S., Morera, L.B., Raya, A., Wahl, G.M., and Izpisúa Belmonte, J.C. (2009). Linking the p53 tumour suppressor pathway to somatic cell reprogramming. Nature *460*, 1140–1144. https://doi.org/10.1038/nature08311.

44. Mohiuddin, I.S., Wei, S.J., and Kang, M.H. (2020). Role of OCT4 in cancer stem-like cells and chemotherapy resistance. Biochim. Biophys. Acta, Mol. Basis Dis. *1866*, 165432. https://doi.org/10.1016/j.bbadis.2019.03.005.

45. Takeda, K., Mizushima, T., Yokoyama, Y., Hirose, H., Wu, X., Qian, Y., Ikehata, K., Miyoshi, N., Takahashi, H., Haraguchi, N., et al. (2018). Sox2 is associated with cancer stem-like properties in colorectal cancer. Sci. Rep. *8*, 17639. https://doi.org/10.1038/s41598-018-36251-0.

46. Qi, X.T., Li, Y.L., Zhang, Y.Q., Xu, T., Lu, B., Fang, L., Gao, J.Q., Yu, L.S., Zhu, D.F., Yang, B., et al. (2019). KLF4 functions as an oncogene in promoting cancer stem cell-like characteristics in osteosarcoma cells. Acta Pharmacol. Sin. *40*, 546–555. https://doi.org/10.1038/s41401-018-0050-6.

47. Egli, D., Rosains, J., Birkhoff, G., and Eggan, K. (2007). Developmental reprogramming after chromosome transfer into mitotic mouse zygotes. Nature *447*, 679–685. https://doi.org/10.1038/nature05879.

48. Halley-Stott, R.P., Jullien, J., Pasque, V., and Gurdon, J. (2014). Mitosis gives a brief window of opportunity for a change in gene transcription. PLoS Biol. *12*, e1001914. https://doi.org/10.1371/journal.pbio.1001914.

49. Chen, G., Gulbranson, D.R., Hou, Z., Bolin, J.M., Ruotti, V., Probasco, M.D., Smuga-Otto, K., Howden, S.E., Diol, N.R., Propson, N.E., et al. (2011). Chemically defined conditions for human iPSC derivation and culture. Nat. Methods *8*, 424–429. https://doi.org/10.1038/nmeth.1593.

50. Beers, J., Gulbranson, D.R., George, N., Siniscalchi, L.I., Jones, J., Thomson, J.A., and Chen, G. (2012). Passaging and colony expansion of human pluripotent stem cells by enzyme-free dissociation in chemically defined culture conditions. Nat. Protoc. *7*, 2029–2040. https://doi.org/10.1038/nprot.2012.130.

51. Cevallos, R.R., Hossain, M.E., Zhang, R., and Hu, K. (2021). Evaluating reprogramming efficiency and pluripotency of the established human iPSCS by pluripotency markers. Methods Mol. Biol. *2239*, 235–249. https://doi.org/10.1007/978-1-0716-1084-8_15.

52. Mi, H., Muruganujan, A., Huang, X., Ebert, D., Mills, C., Guo, X., and Thomas, P.D. (2019). Protocol Update for large-scale genome and gene function analysis with the PANTHER classification system (v.14.0). Nat. Protoc. *14*, 703–721. https://doi.org/10.1038/s41596-019-0128-8.

53. Hu, K. (2021). Become competent in generating RNA-seq heat maps in one day for novices without prior R experience. Methods Mol. Biol. *2239*, 269–303. https://doi.org/10.1007/978-1-0716-1084-8_17.

54. Hu, K. (2020). Become competent within one day in generating boxplots and violin plots for a novice without prior R experience. Methods Protoc. *3*, 64. https://doi.org/10.3390/mps3040064.

55. Geiss, G.K., Bumgarner, R.E., Birditt, B., Dahl, T., Dowidar, N., Dunaway, D.L., Fell, H.P., Ferree, S., George, R.D., Grogan, T., et al. (2008). Direct multiplexed measurement of gene expression with color-coded probe pairs. Nat. Biotechnol. *26*, 317–325. https://doi.org/10.1038/nbt1385.

56. Malkov, V.A., Serikawa, K.A., Balantac, N., Watters, J., Geiss, G., Mashadi-Hossein, A., and Fare, T. (2009). Multiplexed measurements of gene signatures in different analytes using the Nanostring nCounter Assay System. BMC Res. Notes *2*, 80. https://doi.org/10.1186/1756-0500-2-80.

STAR★METHODS

KEY RESOURCES TABLE

REAGENT or RESOURCE	SOURCE	IDENTIFIER
Antibodies		
Anti-OCT4	Cell Signaling	2840; RRID:AB_2167691
Anti -SOX2	BD Pharmingen	561469; RRID:AB_10694256
Anti -NANOG	BD Pharmingen	560109; RRID:AB_1645597
Anti -LIN28	Millipore	MABD53
Alexa fluor 568-donkey-anti-rabbit IgG	Life Technologies	A10042; RRID:AB_2534017
Alexa fluor 488 goat anti-mouse IgG	Life Technologies	A-11029; RRID:AB_2534088
PE-TRA-1-60	BD Pharmingen	560193; RRID:AB_1645539
PE-TRA-1-81	BD Pharmingen	560161; RRID:AB_1645540
PE-SSEA4	BD Pharmingen	560128; RRID:AB_1645533
PE-SSEA3	BD Pharmingen	560237; RRID:AB_1645542
PE-SSEA1	BD Pharmingen	560142; RRID:AB_1645246
PE- anti -ALP (TRA2-49)	R&D Systems	FAB1448P; RRID:AB_883814
TRA-1-60-biotin	eBioscience	13-8863-82; RRID:AB_891594
Biological samples		
RNA samples for RNA-Seq	This study	See Table S2
Chemicals, peptides, and recombinant proteins		
7-AAD(7-aminoactinomycin d)	Life Technologies	A1310
Penicillin-Streptomycin	Gibco	15140122
FBS	Gibco	10437-028
Accutase	ThermoFisher Scientific	A1110501
DMEM/F12	Gibco	12400-024
L-Ascorbic acid 2-phosphate sesquimagnesium salt hydrate	Sigma	A8960-5G
Sodium selenium	Sigma	S5261
Sodium bicarbonate ($NaHCO_3$)	Fisher Scientific	BP328-1
Insulin	CS Bio	CS9212
Transferrin	Sigma	T0665-500MG
tgf beta	Cell Signaling	8915LC
Matrigel (Geltrex)	ThermoFisher Scientific	A1413302
Dulbecco's phosphate-buffered saline (DPBS)	Gibco	21600-044
TrypLE	ThermoFisher Scientific	A1217701
methanol	Fisher Scientific	A412P-4
Tris base	Fisher Scientific	BP152-5
Sodium chloride (NaCl)	Fisher Scientific	BP358-10
Magnesium chloride ($mgcl_2$) hexahydrate	ACROS	41341-5000
N,N-dimethylformamide (DMF)	Fisher Scientific	BP1160-500
4-Nitro blue tetrazolium chloride (NBT)	Thermo Scientific	R0841
5-bromo-4-chloro-3-indolyl-phosphate (BCIP)	Thermo Scientific	34040
Sodium azide (NaN_3)	Sigma-Aldrich	S2002
LB media	Fisher Scientific	BP1426-2

(*Continued on next page*)

Continued

REAGENT or RESOURCE	SOURCE	IDENTIFIER
Ampicillin	Fisher Scientific	BP1760-25
Polyethylenimine (PEI)	Polysciences	24765-2
Polyethylene glycol 6000 (PEG-6000)	EMD Millipore	528877-1KG
Polybrene	Sigma	107689-10G
Paraformaldehyde	Sigma	P6148-500G
Triton x-100	Fisher Scientific	BP151-500
Bovine serum albumin (BSA)	GE Healthcare Life Sciences	SH30574.02
Streptavidin HRP	BD Biosciences	554066
Deposited data		
Bulk RNA-Seq data set	NCBI Gene Expression Omnibus (Edgar et al. 2002)	GSE203207
Critical commercial assays		
Zyppy plasmid MiniPrep kit	Zymo Research	D4020
Quick-RNA miniprep kit	Zymo Research	R1055
Zymoclean gel DNA recovery kit	Zymo Research	D4008
Endofree plasmid Maxi kit	QIAgen	12362
Trizol™ reagent	Invitrogen	15596018
Q5 site-directed mutagenesis kit quick protocol	BioLabs	E0554S
Celltiter96® aqueous one solution cell Proliferation assay (MTS)	Promega	G3582
Click-itTM plust TUNEL assay kits	Invitrogen	C10618
Cell Meter™ live cell caspase 8 binding assay kit	AAT Bioquest	20116
BD Pharmingen tm APC annexin V	BD Biosciences	550474
Metal enhanced dab substrate	Thermo Fisher Scientific	34065
Pierce™ stable peroxide substrate buffer	Thermo Fisher Scientific	34062
Cytotune iPS 2.0	Invitrogene	A16517
nCounter codeset	NanoString	UAB_KH, customized, 53 mitotic genes
Experimental models: Cell lines		
BJ human primary fibroblasts	ATCC	CRL-2522; RRID:CVCL_3653
human embryonic stem cell line H1	WiCell	WA01; RRID:CVCL_9771
Human embryonic stem cell line H9	WiCell	WA09; RRID:CVCL_9773
human iPS cell line generated by BRD3RΔBD1	This study	iPSCdBD1
Lenti-X 293T	Takara	632180
HeLa	ATCC	CCL-2; RRID:CVCL_0030
Recombinant DNA (plasmids)		
BET WT and mutated plasmids	This study	See Table S1
PMD2.G	Didier Trono	Addgene, 12259; RRID:Addgene_12259
PSPAX2	Didier Trono	Addgene, 12260; RRID:Addgene_12260
PLVH-EF1A-GFP-P2A-OCT4	Shao et al. 2016	Addgene, 130692; RRID:Addgene_130692
PLVH-EF1A-GFP-P2A-SOX2	Shao et al. 2016	Addgene, 130693; RRID:Addgene_130693
PLVH-EF1A-GFP-P2A-KLF4	Shao et al. 2016	Addgene, 130694; ID:Addgene_130694
PLVH-EF1A-GFP-P2A-MYC	Shao et al. 2016	Addgene, 130695; RRID:Addgene_130695

(*Continued on next page*)

Continued

REAGENT or RESOURCE	SOURCE	IDENTIFIER
Software and algorithms		
FastQC/0.11.9	FastQC: A Quality Control Tool for High Throughput Sequence Data	https://www.bioinformatics.babraham.ac.uk/projects/fastqc/
MultiQC	MultiQC: summarize analysis results for multiple tools and samples in a single report, Ewels et al. 2016	https://multiqc.info/
SAMtools v1.9	Li et al. 2009	http://www.htslib.org/doc/samtools.html
STAR	Dobin et al. 2013	https://github.com/alexdobin/STAR
HTSeq	Putri et al., 2022	https://htseq.readthedocs.io/en/master/
DESeq2	Love et al., 2014	https://bioconductor.org/packages/release/bioc/html/DESeq2.html
IGV	Robinson et al., 2011	https://software.broadinstitute.org/software/igv/
RStudio	RStudio Team	https://www.rstudio.com/
FlowJo	BD Life Sciences	https://www.flowjo.com/
PANTHER classification system	Mi et al., 2020	http://www.pantherdb.org/
pHeatmap	Raivo Kolde	https://cran.r-project.org/web/packages/pheatmap/index.html
GraphPad Prism 5	GraphPad Software, San Diego, CA, USA	https://www.graphpad.com/
CellSens	Olympus	https://www.olympus-lifescience.com/en/software/cellsens/

RESOURCE AVAILABILITY

Lead contact

Further information and requests for reagents should be directed to and will be fulfilled by the lean contact, Kejin Hu (hukejin@gmail.com).

Materials availability

All unique and stable reagents generated in this study are available from the lead contact with a completed Materials Transfer Agreement. Key plasmids used in this report will be available from Addgene.

Data and code availability

- All RNA-seq data have been deposited at GEO and are publicly available as of the date of publication. Accession code is GEO: GSE203207 (see the key resources table).
- This paper does not report original codes.
- Any additional information required to reanalyze the data reported in this paper is available from the lead contact upon request.

EXPERIMENTAL MODEL AND SUBJECT DETAILS

Human fibroblast cells

We used primary human fibroblast cell line BJ from ATCC (CRL-2522). This fibroblast cell line is not considered as human subject.

METHOD DETAILS

Cell culture

We used Lenti-X 293T Cell Line (Takara Bio, 632180) to package the lentiviral particles. We used HeLa cells to titrate the viral particles. Both Lenti-X 293T and Hela cells were cultured in DMEM/F12 medium (Gibco, 12400-024) supplemented with 10% FBS (Gibco, 10437-028).

We used human primary foreskin BJ fibroblasts as the starting cells in iPSC reprogramming experiments. The BJ fibroblasts (ATCC, CRL-2522) were cultured in DMEM/F12 media supplemented with 10% FBS, and 5 ng/mL human bFGF.

The established iPSC lines and human embryonic stem cells were maintained in E8 medium on Matrigel-coated tissue culture vessels.[49] The E8 medium consists of DMEM/F12, 64 mg/L L-ascorbic acid 2-phosphate sesquimagnesium, 13.6 μg/L sodium selenium, 1.7 g/L sodium bicarbonate, 4 ng/ml FGF2, 20 μg/ml insulin, 10 μg/ml transferrin, and 2 μg/L TGFβ1, at pH 7.4 and an osmolarity of 340 mOsm.

All the above mammalian cells were cultured at 37°C, 5% CO_2, and normoxia. For reprogramming experiments, we cultured the transduced BJ cells in a hypoxia (5% O_2) incubator from days 4 to 15.

Plasmids

We used our lentiviral vector (pLV-EF1a-AcGFP-P2A-) with the EF1a promoter to drive the expression of transgenes, as described previously.[19,33] To facilitate titration of the lentiviral preparations, we co-express GFP along the transgenes via a P2A peptide[5] except for the point mutation constructs, which were generated based on the original BRD3R plasmid from our human kinome library without GFP co-expression.[19] The plasmids used in this study are listed in Table S1. All constructed plasmids were sequenced by Genewiz to verify the correct cloning. Key plasmids will be deposited along with their NTI vector sequence files to the Addgene repository after publication of this work.

Plasmid preparation for virus packaging

We transformed the plasmids into the *Stbl3* competent *E. coli* cells by a heat shock at 42°C for 45 s in a water bath and made a glycerol frozen stock for each construct. From the frozen stock, we streak the bacteria into an ampicillin (100 μg/mL) agar plate using a sterile 1-ml pipette tip. We pick up a single colony and grow overnight in 3 ml of LB broth in the presence of ampicillin (100 μg/mL) at 37°C with constant shaking. We further grow the bacteria from the resulting 3-ml seed culture overnight in 250 ml of LB broth with ampicillin (100 μg/mL) at 37°C with constant shaking. High quality plasmids were prepared from bacteria using the Qiagen EndoFree® Plasmid Maxi Kit (Qiagen, 12362) according to the manufacturer's protocol.

Virus packaging

The day before transfection, 20×10^6 lenti-X 293T cells were seeded in 25 ml of DMEM/F12 media containing 10% FBS (293T medium) in a 150-mm tissue-culture dish. At 24 h post seeding, the used medium was replaced with 25 ml of fresh 293T medium 2 h before transfection. For one transfection, a total of 60 μg of plasmid DNA [22.5 μg packaging (psPAX2, Addgene, 12260), 7.5 μg envelope (pMD2.G, Addgene, 12259), and 30 μg transfer plasmids] were prepared in 3 ml of DMEM/F12 base media in a 15-mL tube. Polyethylenimine (PEI) solution (180 μg, plasmid:PEI = 1:3) was prepared in 3 mL DMEM/F12 media in a 50-mL tube. Then, the DNA mixture was added dropwise into the PEI solution while mixing by pipetting using a 5-mL pipette. The mixture is then incubated for 15 min at room temperature. The plasmids/PEI complex was added dropwise evenly into the 293T cell culture. At 18 hrs post transfection, the spent media were removed, and 25 ml of fresh 293T medium was added to the dish. At 72 hrs post addition of fresh media, the virus-containing medium was collected into a 50-mL tube and the viral particles were concentrated as described in the "virus concentration" section below.

Virus concentration

The virus-containing medium was centrifuged at 400×g for 5 min at 4 °C to remove the cell debris and the resulting supernatant was passed through a 0.4-μm filter (Millipore Sigma, SCHVU01RE). PEG-6000 (stock concentration, 50%) was added to the filtered supernatant at a final concentration of 8.5%. Then, NaCl (stock concentration, 4M) was added to the mixture at a working concentration of 0.4 M. The mixture was incubated at 4 °C for 3–5 h and mixed by inverting the tube 4-5 times every 20–30 min. After incubation, the mixture was transferred to a 50-mL tube and the viruses were pelleted by centrifugation at 4,500×g for 1 hr at 4°C. The supernatant was carefully decanted, and the pellet was resuspended in ice-cold PBS at 1/100 the volume of the original viral supernatant (100-fold concentration) and remained on ice. The concentrated viral stock was divided into 10-μl aliquots. The aliquots were snap frozen by placing the tubes in liquid N_2 immediately after aliquoting. The frozen aliquots were then transferred to a -80°C freezer for

long-term storage. One aliquot of viruses was used to determine the virus titer by flow cytometry based on GFP expression in HeLa cells (see the titration section below).

Titration of lentiviral particles

The titer of the recombinant lentiviral particles was determined as described previously.[33] Briefly, the HeLa cells were cultured in the DMEM/F12 medium supplemented with 10% FBS on a 10-cm culture dish until 80% confluence. The cells were re-seeded into 24-well plates at a density of 2.5×10^4 cells per well. The next day, cells from one well were counted using a haemocytometer and the resulting cell number per well will be used for the titer calculation. The medium was aspirated from the remaining wells and 500 μL fresh media containing polybrene (5 μg/mL) was added into each well. One aliquot of lentiviral stocks was thawed on ice and diluted 100 times with PBS. Different volumes of the diluted viruses (1, 2, 5, 10, and 20 μL) were added to individual wells and mixed by gentle shaking. The cells were cultured overnight at 37°C in 5% CO_2. At 18 hrs post transduction, the medium was replaced with fresh HeLa cell culture media. At 72 hours post medium change, the samples were analyzed with the BD LSRFortessa flow cytometer and the percentage of GFP positive cells were calculated using the FlowJo software. The titer was calculated using the following formula in TU/mL (transduction units per milliliter): $TU/mL = \frac{N\times\%\ GFP\times D_f\times1000}{100\times V_{uL}}$, $V_{\mu L}$, volume of diluted virus in μL; N, cell number at the time of virus addition; %GFP, percentage of GFP positive cells; D_f, the dilution factor.

Cell culture and reprogramming

The reprogramming of human foreskin BJ fibroblasts into induced pluripotent stem cells (iPSCs) were performed according to the previously described protocol.[19,33] Briefly, the BJ fibroblasts (ATCC, CRL-2522) were cultured in DMEM/F12 media supplemented with 10% FBS and 5 ng/ml human bFGF. For reprograming, the BJ fibroblasts were seeded into 6-well plate at 5×10^4 cells per well or 12-well plate at 2.5×10^4 cells per well. The next day, cell number of 1 well were counted and the MOI to be used was calculated accordingly. The media was aspirated and fresh media along with premixed OSK (OCT4, 8 MOI; SOX2, 5 MOI; KLF4, 5 MOI) viruses were added along with individual test BET viruses (MOI, 3) into respective wells. The next morning, viruses were removed by replacing virus-containing medium with fresh fibroblast medium. At 24 h post virus removal, the transduced cells were reseeded from one well into 3 Matrigel-coated wells of the same size. The next day, fibroblast medium was replaced with E7 media (E8 media minus TGFβ). From day 15 on, E8 medium was used and changed daily. E8 medium is composed of DMEM/F12, 64 mg/L L-ascorbic acid 2-phosphate sesquimagnesium, 13.6 μg/L sodium selenium, 1.7 g/L sodium bicarbonate, 4 ng/ml FGF2, 20 μg/ml insulin, 10 μg/ml transferrin and 2 μg/L TGFβ1 (pH 7.4, osmolarity 340 mOsm). On day 18-21, reprogramming efficiencies were evaluated by staining the reprogrammed colonies for alkaline phosphatase as described in a separate section. Each set of test and control reprogramming experiments was conducted on the same days by the same scientist using the same number of cells from the same preparation of starting cells in the same size of cell culture vessels (6-well or 12-well). The number of colonies from control and test reprogramming are compared, and fold differences are calculated. Reprogramming percentage based on the number of starting cells were also calculated. Each set of experiments were independently conducted at least 3 times.

The established iPSC lines were maintained in E8 medium on Matrigel-coated tissue culture vessels using the standard procedure.[50]

Reprogramming with Sendai vectors

Human fibroblasts BJ cells at passage 3 were cultured till 80% confluency and then passaged into 12-well plates at a density of 1.4×10^4 cells per cm^2. The next day, cells from one well were detached with TrypLE and counted to calculate the amounts of Sendai vectors required. We conducted the Sendai reprogramming following the manufacture's instruction. We used a MOI of 5 for KOS, 3 for KLF4 and 2 for MYC. Additionally, we transduced the cells with either GFP control vector or BRD2ΔBD1ΔET mutant vector at MOI 3. The transduction mix was prepared in BJ expansion medium supplemented with 4 μg/mL polybrene. We incubated the cells with the aforementioned transduction mix for 18 hours, then, washed with PBS, and fed with fresh BJ expansion medium. At day 3 after transduction, the cells were split into Geltrex-coated wells at a density of 7×10^3 cells per cm^2. Cells were re-fed every other day with E7 medium for 12 days. At that point, colonies were big enough for analysis by TRA1-60 antibody staining.

Alkaline phosphatase (ALP) staining

Alkaline phosphatase staining was performed as described previously.[51] Briefly, the reprogrammed colonies were fixed with pre-cooled 100% methanol for 10 mins at room temperature. After fixation, methanol was aspirated and the fixed colonies were then washed with DPBS (room temperature) two times, and then with tris-buffered saline (TBS), pH 9.0 once (room temperature). The 5-bromo-4-chloro-3-indolyl-phosphate (BCIP; final concentration, 0.15 mg/mL) was mixed with 4-nitro blue tetrazolium chloride (NBT; final concentration, 0.30 mg/mL) in a falcon tube. The BCIP/NBT solution was added to the fixed reprogrammed cells and incubated for 15-25 mins in dark at RT. When the staining is complete, the BCIP/NBT solution was aspirated, and the stained cells were washed with DPBS once. The stained cells can be stored in DPBS containing 0.05 % sodium azide (NaN_3) before imaging and colony counting. The stained cells were scanned by a photo scanner (Epson perfection v700 photo).

TRA1-60 staining of iPSC colonies

Reprogramming/reprogrammed cells at day 20 (lentiviral system) or day 12 (Cytotune 2.0 system) were washed one time with PBS and then fixed using ice-cold methanol, which was pre-cooled in a -20°C freezer overnight. After incubation with methanol for 10 minutes, cells were washed with PBS and then blocked with 2% BSA in PBS for 1 hour. After blocking, cells were incubated with TRA1-60 antibody (diluted in blocking solution) overnight at 4°C. Then, cells were washed 3 times with PBS and incubated with streptavidin-HRP (diluted in blocking solution) for 2 hours at room temperature. Cells were then washed again 3 times with PBS, and then incubated with 1× DAB substrate (Thermo Fisher Scientific) diluted in 1× Peroxide Substrate Buffer (Thermo Fisher Scientific), for 10 minutes at room temperature. DAB substrate solution was removed and replaced with PBS. Dark brown colonies were counted as positive for Podocalyxin/TRA-1-60.[34]

Immunocytochemistry and microscopy

Cells were fixed with 4% paraformaldehyde in PBS at room temperature for 15 min. After washed three times with PBS, the fixed cells were then blocked with 0.1% Triton X-100, 1% BSA in PBS at room temperature for 1 hr. The blocked cells were then incubated with the diluted primary antibody overnight at 4 °C (See list of antibodies in the key resources table). The next morning, the cells were washed five times with TBS-T (Tris-buffered saline, pH 7.0, 0.1% tween-20) and then incubated with an appropriate secondary antibody at room temperature in the dark for 1 h. After washed with PBS, cell nuclei were stained with 1 μg/ml DAPI at room temperature for 5–10 min. The images of the stained cells were acquired using a fluorescence microscope, Olympus IX51 equipped with the CellSens software.

Detection of pluripotency surface markers by flow cytometry

We used flow cytometry to detect the pluripotency surface markers of the established human iPSC lines, as described previously.[51] Briefly, the established iPSC lines were cultured with E8 media. When iPSC colonies reached 80–85% confluence, the medium was aspirated, and the cells were detached with a treatment with pre-warmed Accutase for 5 min at 37°C. The resulting cells were harvested by centrifugation at 300×g for 5 min at 4°C. The cell pellet was resuspended in FACS buffer (PBS supplemented with 2% FBS, 1 mM EDTA) and incubated with PE-conjugated SSEA1, SSEA3, SSEA4, TRA1-60, TRA1-81, and ALP antibodies (See list of antibodies in the key resources table) for 1 hr on ice in the dark. The stained cells were then washed with FACS buffer once by a centrifugation procedure, and then resuspended in FACS buffer. The dead cells were stained with 7-AAD (final concentration, 0.5 μg/mL) for 5 min on ice before analyses with the BD LSRFortessa Cell Analyzer. The data were analyzed using FlowJo.

TUNNEL assay

Late-stage apoptosis was assayed using Click-iT Plus TUNEL Assay kit (Invitrogen, C10618) following the manufacturer's protocol. Briefly, BJ cells of passage 3 were thawed and cultured in fibroblast medium for at least one passage before used in the experiments. The recovered cells were then passaged into 6-well plates at a density of 1×10^5 cells per well. The next day, the cells were transduced with the corresponding lentiviral particles in fibroblast media supplemented with 5 μg/mL hexadimethrine bromide (Polybrene). At 18 hours post addition of viruses into the media, the spent transduction media were removed, and the cells were washed one time with PBS before addition of fresh media. The next day, the transduced cells were detached using TrypLE and then passaged into Geltrex-coated, 8-well coverslips at a density of 1×10^4 cells per well. Cells were allowed to grow for two more days in E7 medium or fibroblast

medium and then fixed with 4% formaldehyde. After fixation, cells were permeabilized with 0.25% Triton X-100 in PBS for 20 minutes. Cells were washed twice with deionized water and then 100 μL of TdT reaction buffer was added to each well. Cells were incubated for 10 minutes at 37°C. After incubation, 100 μL of freshly prepared TdT reaction mixture was added to each well and the cells were incubated for 1 hour at 37°C. After incubation, cells were washed twice with 3% BSA in PBS and then 100 μL Click-iT Plus TUNEL reaction cocktail was added to each well. Coverslips were incubated for 30 minutes at 37°C, protected from light. After TUNEL reaction, cells were washed twice with 3% BSA in PBS and the cell nuclei were stained with 200 uL of 1×DAPI solution (ThermoFisher Scientific, 62248) for 15 minutes. The resulting cells were washed twice with PBS before analyses with epi-fluorescence microscopy.

Caspase 8 activity assay

Activated caspase 8 was assayed using Cell Meter^{TM} Live Cell caspase 8 Binding Assay kit (AAT Bioquest, 20116) following manufacturer's guidelines. Briefly, fresh BJ cells at early passages were passaged into 6-well plates at a density of 1×10^5 cells per well. The next day, the cells were transduced with the corresponding lentiviral vectors in fibroblast medium supplemented with 5 μg/mL Polybrene. At 18 hours post addition of viruses, the cells were washed one time with PBS and fresh medium was added. Transduced cells were cultured for 3 more days with daily medium change. At day 4 after transduction, the cells were washed one time with PBS and detached using 1 mL of Versene solution (Gibco, 15040066) for 5 to 10 minutes. Harvest the cells by standard centrifugation, and the cellular pellets were gently resuspended in 500 μL of fresh medium supplemented with 1× iFluor 647-LETD-FMK solution. The cells were transferred into 5-mL round-bottom FACS tubes, and incubated for 1 hour at 37°C. After incubation, the cells were washed twice with wash buffer supplied in the kit. After washing, the cells were resuspended in 500 μL of wash buffer. Cell fluorescence was detected using BD LSRFortessa Flow Cytometer using APC channel. The activated caspase 8 were analyzed using FlowJo software.

Annexin V staining

Apoptosis was assayed using APC Annexin V (BD Biosciences, 550474), following manufacturer's guidelines. Briefly, BJ cells at early passages were seeded into 6-well plates at a density of 1×10^5 cells per well. The next day, the cells were transduced with the corresponding lentiviral particles in fibroblast medium supplemented with 5 μg/mL Polybrene. After transduction for 18 hours, the cells were washed one time with PBS and fresh medium was added. Transduced cells were cultured for 3 more days with daily medium change. At day 4 after transduction, the cells were washed one time with PBS and detached using 1 mL of Versene solution (Gibco, 15040066) for 5 to 10 minutes. The detached cells were collected by standard centrifugation and the cellular pellets were gently resuspended in 100 μL of Binding Buffer, composed of 0.1 M HEPES (pH 7.4), 1.4 M NaCl, 25 mM $CaCl_2$, and supplemented with 5 μL APC-conjugated Annexin V and 0.25 μg 7-AAD (ThermoFisher Scientific, A1310). Cells were incubated for 15 minutes at 25°C in the dark. After incubation, 500 μL of 1× Binding Buffer was added and transferred into each 5-mL FACS tube. Cell florescence was detected using BD Fortessa flow cytometer using the APC and PE-Cy5 channels. Annexin V/apoptosis was analyzed using FlowJo software.

Cell cycle analyses

We transduced cells as described in the reprogramming experiments, and cell cycles were analyzed 72 hours post virus removal that is the same time we extracted total RNA for RNA-seq experiments. We harvested the cells using TrypLE and pelleted them by a centrifugation at 500×g for 5 min. The cells were washed with PBS one time with the standard centrifugation procedure, and the resulting cell pellet was resuspended in 50 μL of PBS. Add 4.5 ml of ice-cold 100% methanol dropwise into the cell suspension while vertexing and then fix them on ice for 30 min. Spin down the cells and discard the methanol. Wash the cells one time with 5 ml of PBS by the centrifugation procedure. Resuspend the cells in 500 μL of PBS buffer supplemented with 25 μg/ml 7-AAD and 200 μg/ml of RNAse A. Stain the cells in dark for 30 min at room temperature. Acquire the cell cycle profile data using a flow cytometer and analyze the cell cycle profiles using FlowJo.

Cell viability and cytotoxicity assay

Cell viability and cytotoxicity was assayed using Celltiter 96® AQueous One Solution (Promega, G3582), following the manufacturer's guidelines. Briefly, BJ cells were transduced with GFP control or with the OSK reprogramming factors and either GFP, BRD2ΔBD1ΔET, BRD3ΔBD1ΔET, or BRD4SΔBD1ΔET. Cells

were passaged at day two (24 hours post transduction) into Geltrex-coated 96-well plates in triplicate at a density of 1×10^4 cells per well. Cells were then assayed every 48 hours from the time of passaging. For each assay, cells were treated in 100 μL per well of fresh fibroblast medium supplemented with 10 uL of CellTiter96 staining reagent for 2 hours at 37°C. We took 50 μL of the reaction solution/medium per well and transferred the solution into wells of a clean 96-well plate. Reaction was stopped immediately by adding 10 uL of 10% SDS to each 50-μL aliquot. Readings were recorded using a Nanodrop devise (option UV-Vis, Wavelength 490 nm, and baseline correction 750 nm). Fibroblast medium containing CellTiter96 staining reagent without any cells was used as blank control.

Teratoma assays

The Institutional Animal Care and Use Committee (IACUC) at the University of Alabama at Birmingham (UAB) approved the animal protocols. The iPSCs were cultured in E8 medium on Matrigel-coated vessels. When the cells reached 80% confluence, the iPSC colonies were harvested using EDTA dissociation solution (0.5 mM EDTA in calcium/magnesium-free PBS) and pelleted by centrifugation at 300×g for 5 mins at 4°C. The supernatant was discarded, and the pellet was resuspended with Matrigel at a final concentration of 50%. We injected 2×10^6 of iPSCs subcutaneously into one flank of a mouse (*NOD.Cg-Prkdcscid Il2rgtm1Wjl/SzJ*, NSG mice, Jackson Laboratory, 005557; age of 6-week or older; male or female). After 6 to 8 weeks post injection, teratoma was collected surgically. The harvested teratoma were immediately submerged in 4% formaldehyde for fixation at room temperature. Histology was performed in the Comparative Pathology Laboratory at UAB.

Karyotyping

The generated iPSCs were karyotyped by Cell Line Genetics (Madison, WI, USA). We seeded the iPSCs in a T25 flask in E8 media supplemented with ROCK inhibitor, Y-27632 or thiazovivin, and shipped it overnight to the Cell Line Genetics.

RNA preparation for RNA-seq

The BJ fibroblasts (ATCC, CRL-2522) were cultured in six-well plates at a density of 2×10^5 cells per well. At 24 hrs post seeding, cells from one well were counted using a haemocytometer and multiplicity of infection (MOI) was calculated accordingly. The medium was aspirated from the remaining wells and 2 mL of fresh medium containing polybrene (final concentration, 5 μg/mL) was added to the wells. The viruses were added into respective wells. At 18 hrs post addition of viruses, the media containing the residual viruses were removed and fresh fibroblast medium was added. At 72 hrs from virus removal, the spent medium was removed and 1 mL of TRIzol was added directly to each well. RNA was extracted using the manufacturer's protocol. After extraction, the RNA was further purified using Quick RNA Miniprep kit (Zymo Research, R1055), according to the manufacturer's protocol.

RNA-seq

We sent our total RNA to Novogene for RNA-seq. Briefly, the library was prepared using the NEBNext Ultra II RNA Library Prep by Illumina. Human mRNAs were purified by oligo(dT) beads. Non-stranded protocol was used. The purified mRNAs were fragmented randomly in fragmentation buffer and the first-strand cDNA was synthesized using random hexamer primers and the M-MuLV Reverse Transcriptase (RNase H^-). The second strand is subsequently generated by dNTPs, DNA polymerase I and RNase H. Double-stranded cDNA molecules were purified by AMPure XP beads and overhanging ends were repaired to blunt ends by exonuclease/polymerase. After 5′ phosphorylation and 3′ adenylation, the cDNAs were ligated with P5/P7 sequencing adapters to prepare for hybridization. In order to select the insert fragment of preferentially 150-200 bp in length, the modified libraries are purified with AMPure XP system (Beckman Coulter, Beverly, USA). The final library is ready after PCR amplification and products purification by AMPure XP beads.

The sequencing was conducted on Novaseq6000 S4 Illumina using the paired-end protocol. The raw read counts ranged from 23.38×10^6 to 52.65×10^6, and the uniquely mapped read counts ranged from 25.29×10^6 to 48.72×10^6 with the uniquely mapped rates from 85.13% to 96.41% (Table S2). We also re-used 7 RNA-seq samples previously deposited by our laboratory (Table S3).

Bioinformatics

The detailed step-by-step procedures of the RNA-seq analysis pipeline have been described in full.[42] Briefly, FASTQ files of RNA-seq were uploaded to the UAB high-performance computing cluster, Cheaha. We conducted the quality control using the FastQC module. The sequenced fragments were aligned to human reference genome (GRCh38, release 105) using the STAR aligner, and the aligned BAM files were sorted and indexed using the SAMtools software. The aligned data were counted to features using the *htseq-count* command of the HTSeq module. The differential expressions (DE) were analyzed using the DESeq2 package on the RStudio server of the Cheaha cluster.

DE gene lists were analyzed for gene ontology (GO) enrichments using the web-based PANTHER tools.[52] Human annotation data set of "GO biological process complete" along with other data sets (for example, Reactome Pathways) was used for statistical overrepresentation test of gene lists using the default "Fisher's Exact" setting. Stress/stimulus response GO terms were selected from the enriched GO term lists of "biological process" using the key words of "response", "stress" and "stimulus".

All RNA-seq raw data (FASTQ files) and the normalized read counts have been deposited to GEO database with the accession code of GSE203207.

The RNA-seq alignment tracks were visualized on Integrative Genomics Viewer (IGV) server of Cheaha. Heat maps were prepared using the Pheatmap package on our RStudio server as described.[53] Boxplots were prepared with RStudio as described previously.[54] PCA was conducted on RStudio using the DESeq2 package.

Quantitate transcriptional turbulence caused by the yamanaka factors

We have previously developed a simple method to quantitate overall transcriptional differences between two conditions or cell types.[35] Briefly, the transcriptional difference at a selected significant level for a gene can be calculated: $G_d = \log2(FC)$. Here, G_d is the transcriptional difference for an individual gene while FC is the fold change of that gene. The overall transcriptional difference are the sum of the up-difference and the absolute down-difference, both of which can be calculated with:

$$Td = \sum_{i=1}^{n} log\,2(FCi)$$

T_d is the up- or down-transcriptional difference at the transcriptome level with a unit of LFC (log2 fold change); FC_i is fold change in gene i; n is the total number of genes that are up- or down-regulated significantly. The quantitative differences can be visualized using waterfall plots. This method was used in this study to quantitate the degree of transcriptional turbulence by the Yamanaka transcriptional factors. We additionally tallied and compared the number of DE genes as a measurement of transcriptional turbulences.

NanoString nCounter™ quantification of gene expression

To verify the RNA-seq results we used another high-throughput technology, NanoString's nCounter™ Analysis System.[55,56] We chose the entire set of 53 mitotic genes upregulated by the DN forms of the three BET proteins. A custom probe set (CodeSet Name, UAB_KH_9799) for the 53 mitotic target genes and 6 reference genes (*COX11*, *COX19*, *ERCC3*, *GANAB*, *CCNY*, and *MRFAP1*) (Table S15). The CodeSet was designed and validated by NanoString such that each target-specific probe would cover all known transcript isoforms of a particular gene. The contiguous target region of each gene is 100 bp in length, 50 bp of which are target of the capture probe, and the other 50 bp of which is the target of the reporter probe. We compared the expression of these 53 genes across 7 experimental conditions with duplicates for each condition. The 7 conditions are: OSK-GFP, OSK-BRD2, OSK-BRD3, OSK-BRD4S, OSK-BRD2ΔBD1ΔET, OSK-BRD3ΔBD1ΔET, and OSK-BRD4SΔBD1ΔET. Assay was performed at the UAB NanoString Laboratory, following the NanoString protocols from the manufacturer. Briefly, for each RNA sample 100 ng of total RNA was hybridized to the UAB_KH_C9799 probe set overnight (17 hours) at 65°C. The hybridized samples were loaded on the nCounter Prep Station with automatic processing; nCounter Master Kit reagents were added to remove the excess probes, and the purified target/probe complexes were immobilized in the nCounter cartridge for data collection. Digital quantification of the color-coded barcodes on the surface of the cartridge was carried out in the nCounter Digital Analyzer.

The raw counts of expression data were analyzed using the Rosalind web-based platform. Briefly, Rosalind normalized the counts according to 6 positive and 8 negative spike-in control probes and the geometric mean of the five housekeeping genes. First, the geNorm algorithm (which looks for stable expression) is used to select suitable housekeeping genes (HKGs) from among all the HKGs in the panel, then for each sample, the geometric mean of the selected housekeepers is calculated (sample HK mean). Second, an experiment-wide HK geometric mean is calculated by taking the geometric mean of all the sample HK means and a per-sample normalization factor is calculated by dividing the experiment-wide mean by the HK mean for that sample. Finally, all counts in a sample are multiplied by the per-sample normalization factor for that sample, and the base-2 logarithm of each normalized count is taken for graphing the differential expressed genes.

QUANTIFICATION AND STATISTICAL ANALYSES

The GraphPad Prism 5 software was used to test statistical significance. Student unpaired t-test was performed to compare the data between two groups. For multiple comparison, one way ANOVA was performed followed by Tukey post-hoc tests. The p-value less than 0.05 ($p < 0.05$) was considered as statistically significant.

For RNA-seq differential expression (DE) analyses, we used the DESeq2 package to conduct the statistics. The threshold for DE gene list generation is 1.5-fold changes at the $q < 0.05$ level. A gene is considered not expressed when its average normalized read counts is less than 50 as we previously proposed.[35]